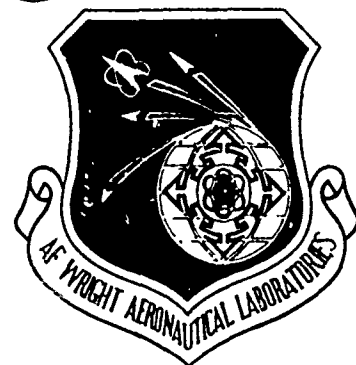


AD-A151 017

AFWAL-TR-84-3080
VOLUME V



**ADVANCED LIFE ANALYSIS
METHODS - Executive Summary
and Damage Tolerance Criteria
Recommendations for Attachment Lugs**

K. Kathiresan

**Lockheed-Georgia Company
Marietta, Georgia 30063**

T. R. Brussat

**Lockheed-California Company
Burbank, California 91520**

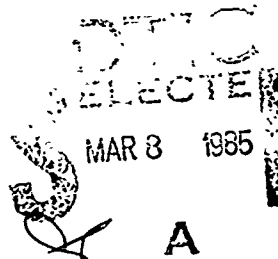
September 1984

Final Report for Period 3 September 1980 to 30 September 1984

Approved for Public Release; Distribution Unlimited.

DMC FILE COPY

**Flight Dynamics Laboratory
Air Force Wright Aeronautical Laboratories
Air Force Systems Command
Wright-Patterson Air Force Base, Ohio 45433**



A

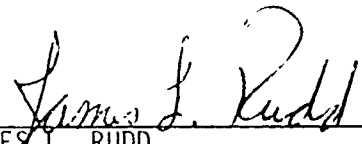
85 02 26 05 9

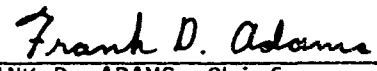
NOTICE

When Government drawings, specifications, or other data are used for any purpose other than in connection with a definitely related Government procurement operation, the United States Government thereby incurs no responsibility nor any obligation whatsoever; and the fact that the government may have formulated, furnished, or in any way supplied the said drawings, specifications, or other data, is not to be regarded by implication or otherwise as in any manner licensing the holder or any other person or corporation, or conveying any rights or permission to manufacture use, or sell any patented invention that may in any way be related thereto.


This report has been reviewed by the Office of Public Affairs (ASD/PA) and is releasable to the National Technical Information Service (NTIS). AT NTIS, it will be available to the general public, including foreign nations.

This technical report has been reviewed and is approved for publication.


JAMES L. RUDD
Project Engineer


FRANK D. ADAMS, Chief
Structural Integrity Branch
Structures & Dynamics Division

FOR THE COMMANDER


ROGER J. HEISTROM, Colonel, USAF
Chief, Structures & Dynamics Division

"If your address has changed, if you wish to be removed from our mailing list, or if the addressee is no longer employed by your organization please notify AFWAL/FIBE, W-PAFB, OH 45433 to help us maintain a current mailing list".

Copies of this report should not be returned unless return is required by security considerations, contractual obligations, or notice on a specific document.

Unclassified

SECURITY CLASSIFICATION OF THIS PAGE

REPORT DOCUMENTATION PAGE

1a. REPORT SECURITY CLASSIFICATION Unclassified			1b. RESTRICTIVE MARKINGS		
2a. SECURITY CLASSIFICATION AUTHORITY			3. DISTRIBUTION/AVAILABILITY OF REPORT Unclassified/Unlimited		
2b. DECLASSIFICATION/DOWNGRADING SCHEDULE					
4. PERFORMING ORGANIZATION REPORT NUMBER(S) LG82ERO117-V			5. MONITORING ORGANIZATION REPORT NUMBER(S) AFWAL-TR-84-3080, Volume V		
6a. NAME OF PERFORMING ORGANIZATION Lockheed-Georgia Company		6b. OFFICE SYMBOL (If applicable)	7a. NAME OF MONITORING ORGANIZATION Air Force Wright Aeronautical Laboratories (AFWAL/FIBEC)		
6c. ADDRESS (City, State and ZIP Code) 86 South Cobb Drive Marietta, Georgia 30063			7b. ADDRESS (City, State and ZIP Code) Wright-Patterson Air Force Base Ohio 45433		
8a. NAME OF FUNDING/SPONSORING ORGANIZATION AFWAL/FIBEC		8b. OFFICE SYMBOL (If applicable)	9. PROCUREMENT INSTRUMENT IDENTIFICATION NUMBER F33615-80-C-3211		
8c. ADDRESS (City, State and ZIP Code) Wright-Patterson Air Force Base Ohio 45433			10. SOURCE OF FUNDING NOS.		
			PROGRAM ELEMENT NO. 62201F	PROJECT NO. 2401	TASK NO. 01
					WORK UNIT NO. 38
11. TITLE (Include Security Classification) See Reverse					
12. PERSONAL AUTHOR(S) Kathiresan, K., Lockheed-Georgia Co., Marietta, Georgia Brussat, T.R., Lockheed-California Co., Burbank, California					
13a. TYPE OF REPORT Final Report		13b. TIME COVERED FROM Sept. 80 to Sept. 84		14. DATE OF REPORT (Yr., Mo., Day) 84-9-17	
				15. PAGE COUNT 72	
16. SUPPLEMENTARY NOTATION This is the 5th volume of a 6 part report on					
17. COSATI CODES			18. SUBJECT TERMS (Continue on reverse if necessary and identify by block number)		
FIELD	GROUP	SUB. GR.	Attachment Lugs, Aircraft, Damage Tolerance, Cracking Data Survey, NDI Assessments, Analysis Methods, Crack Growth Predictions, Experimental Testing, Correlation.		
1	3	1			
1	3	3			
19. ABSTRACT (Continue on reverse if necessary and identify by block number) This report is Vol. V of a 6-part final report on the work conducted under AFWAL contract No. F33615-80-C-3211. The objective of this research program is to develop the design criteria and analytical methods necessary to ensure the damage tolerance of aircraft attachment lugs. This program consisted of seven tasks, proceeding logically from an extensive cracking data survey and assessment of nondestructive inspection capabilities, through analysis methods development and evaluation, to the recommending of the damage tolerance design criteria for aircraft attachment lugs. Volumes I-IV provide the results of the first six tasks. The results of the cracking data survey and nondestructive inspection capabilities assessment (Tasks I and II) are reported in Vol. I. The developed analytical methods for predicting residual strength and crack growth behavior in attachment lugs are presented in Vol. II. The results of analytical predictions (Task IV), experimental					
20. DISTRIBUTION/AVAILABILITY OF ABSTRACT UNCLASSIFIED/UNLIMITED <input checked="" type="checkbox"/> SAME AS RPT. <input type="checkbox"/> DTIC USERS <input type="checkbox"/>			21. ABSTRACT SECURITY CLASSIFICATION Unclassified		
22a. NAME OF RESPONSIBLE INDIVIDUAL J. L. Rudd			22b. TELEPHONE NUMBER (Include Area Code) (513) 255-6104		22c. OFFICE SYMBOL AFWAL/FIBEC

11. TITLE

ADVANCED LIFE ANALYSIS METHODS - Executive Summary and Damage Tolerance
Criteria Recommendations for Attachment Lugs (Unclassified)

18. (continued)

Results and Conclusions, Criteria Assessment, Recommendation of Initial Flaw Size,
Single Lugs, Redundant Lugs

19. (continued)

testing (Task V) and analytical-experimental correlations (Task VI) are reported in Vol.
III. Vol. IV contains the tabulation of raw experimental data generated under Task V.

This volume presents a ^{SUMMARIZES} summary of results for the first six tasks and recommends the
initial flaw requirements for damage tolerance design criteria for aircraft attachment
lugs, which were developed in Task VII. Vol VI -

The last volume of this final report, Vol. VI, is the user's manual for the computer
program "LUGRO" for the prediction of crack growth behavior in attachment lugs.

Unclassified

FOREWORD

This is Volume V of six final report volumes on Contract F33615-80-C-3211, "Advanced Life Analysis Methods." The work reported herein was conducted jointly by Lockheed-Georgia Company and Lockheed-California Company under contract with Air Force Wright Aeronautical Laboratories, Wright-Patterson AFB. J. L. Rudd is the Air Force project leader.

The authors wish to thank F. M. Conley and J. O. Wilson of Lockheed-Georgia Company and E. K. Walker of Lockheed-California Company for their interest in and contribution to the development of the damage tolerance criteria for attachment lugs recommended in this report. The contributions of T. M. Hsu (presently with Gulf E & P Co.) to the overall program are also gratefully acknowledged.

✓

ALL INFORMATION CONTAINED HEREIN IS UNCLASSIFIED

DATE 11/10/01 BY 1045

11/10/01

Dist

A1



TABLE OF CONTENTS

<u>Section</u>	<u>Title</u>	<u>Page</u>
I.	INTRODUCTION AND SUMMARY	1
II.	SERVICE CRACKING SURVEY AND NDI ASSESSMENT	5
	1. Causes of Service Cracking and Service Failures	
	2. Crack Type, Shape and Location	
	3. Crack Multiplicity	
	4. Critical and Inspectable Crack Sizes	
III.	CRACK GROWTH ANALYSIS METHODS	11
	1. Stress Intensity Factors for Straight Lugs	
	2. Stress Intensity Factors for Tapered Lugs	
	3. Fatigue Crack Growth Computation	
	4. Revised Analysis Methods	
IV.	CRACK GROWTH TEST RESULTS AND CORRELATIONS	29
	1. Experimental Program	
	2. Results and Conclusions from Group I Tests	
	3. Results and Conclusions from Group II Tests	
V.	CRITERIA ASSESSMENT	55
	1. Initial Flaw Type and Size for Lugs	
	2. Flaw Multiplicity for Redundant Lugs	
	3. Summary of Initial Flaw Recommendations	
	REFERENCES	63

LIST OF FIGURES

<u>Figure</u>	<u>Title</u>	<u>Page</u>
1-1	Roadmap of the Program	2
2-1	Causes of Failure for Lugs in Service	6
2-2	Results of 55 Lugs that Failed in Service by Fatigue Crack Growth	6
2-3	Critical Crack Sizes After Fatigue Crack Growth in 35 Service Failed Lugs (Air Force ALC Data Only)	8
3-1	Comparison of Stress Intensity Factors Computed Using the Compounding, Weight Function and Cracked Finite Element Methods	15
3-2	Two-Parameter Corner Crack Stress Intensity Factor Formulas	17
3-3	Comparison of Corner Crack Correction Factors at the Lug Surface by the Three Methods	19
3-4	Fatigue Critical Locations of Tapered Lugs Subjected to Various Load Orientations	20
3-5	Normalized Stress Intensity Factors for Single Through-the-Thickness Cracks Emanating from a Tapered Lug Subjected to a Pin Loading Applied in -45° and its Reversed Directions ($R_0/R_1 =$ 2.25)	24
3-6	Normalized Stress Intensity Factors for Single Through-the-Thickness Cracks Emanating from a Tapered Lug Subjected to a Pin Loading Applied in -90° and its Reversed Directions ($R_0/R_1 =$ 2.25)	25
3-7	Comparison of Calculated Tangential Stress on the Eventual Crack Path in the Simulated Wing- Pylon Lug, Assuming Lug-Bushing Separation or Intimate Contact	28
4-1	Geometries of Group I and Group II Test Specimens	31
4-2	Accuracy of Residual Strength Predictions for Group I Tests	34

LIST OF FIGURES (Cont'd)

<u>Figure</u>	<u>Title</u>	<u>Page</u>
4-3	Through-the-Thickness Crack Growth Data and Prediction, Aluminum Lug, $R_o/R_i = 2.25$, $\sigma_o = 6$ ksi, $R = 0.1$	36
4-4	Corner Crack Growth Data and Prediction, Aluminum Lug, $R_o/R_i = 3.0$, $\sigma_o = 6$ ksi, $R = 0.1$	37
4-5	Corner Crack Growth Data and Prediction, Aluminum Lug, $R_o/R_i = 3.0$, $\sigma_o = 15$ ksi, $R = 0.1$	39
4-6	Corner Crack Growth Data and Prediction, Steel Lug, $R_o/R_i = 2.25$, Cargo Spectrum Loading	40
4-7	Accuracy of Prediction of Total Crack Growth Life for Group I Tests	42
4-8	Results of Pin-Clearance Study, Axially-Loaded Straight Lugs	43
4-9	Effect of Lug Geometry on Crack Growth Life	45
4-10	Comparison of Two Analysis Methods for Lugs with Shrink-Fit Bushings	46
4-11	Crack Profiles for Steel Tapered Lugs Loaded in the -90 Degree Direction	47
4-12	Crack Curving and Secondary Cracks in Specimens S3-A-1 through -4	48
4-13	Correlation of Test and Predicted Crack Growth Lives Before Transition for a Corner Crack in Thick Straight Lugs	50
4-14	Fracture Surface of Simulated Wing-Pylon Lug Specimen R2-E-2	51
4-15	Crack Growth in Simulated Wing-Pylon Specimens R2-E-1 and R2-E-2	52
4-16	Accuracy of Prediction of Total Crack Growth Life for Group II Tests	54
5-1	The Equivalence of a Deep, Sharp Scratch and a 0.005-Inch Corner Crack	59

LIST OF TABLES

<u>Table</u>	<u>Title</u>	<u>Page</u>
3-1	Normalized Unflawed Stress Distribution Along x-Axis for Straight Attachment Lugs	13
3-2	Normalized Stress Intensity Factors for Single Through-the-Thickness Cracks in Straight Attachment Lugs Using Cracked Finite Element Method	14
3-3	Normalized Unflawed Stress Distribution Along x-Axis for Tapered Attachment Lugs	22
3-4	Normalized Stress Intensity Factors for Single Through-the-Thickness Cracks in Tapered Attachment Lugs Using Cracked Finite Element Method	23
4-1	Scope of Group I Residual Strength and Crack Propagation Tests	30
4-2	Scope of Group II Crack Propagation Tests	33
5-1	Recommended Damage Tolerance Initial Flaw Size Requirements for Lugs	62

SECTION I

INTRODUCTION AND SUMMARY

Attachment lugs can be some of the most fracture critical components in aircraft structure, and the consequences of structural lug failure can be very severe. Therefore a 42-month research program was initiated in 1980 to develop the design criteria and analytical methods necessary to ensure the damage tolerance of aircraft attachment lugs. The program, summarized in Figure 1-1, consisted of seven tasks, proceeding logically from an extensive cracking data survey and assessment of nondestructive inspection (NDI) capabilities, through analysis methods development and evaluation, to the recommending of damage tolerance design criteria for lugs. This is Volume V of a six-volume sequence of final reports (References [1] - [5]) covering these tasks.

Task I involved a survey of structural cracking data such as the initial flaw size, shape and location which occur in aircraft attachment lugs. Sources for these data included the open literature, available Lockheed data, and visits to the five Air Force Air Logistics Centers (ALC's). The types of aircraft structure used to obtain these data include service aircraft, full-scale component tests, and lug coupon specimens.

Task II assessed the current NDI capability to find these flaws or cracks. This assessment was based upon information obtained from the open literature, available Lockheed NDI data and experience, and Air Force ALC data. The NDI techniques capable of finding flaws in attachment lugs and the flaw sizes these techniques are capable of finding were identified. The results obtained from Tasks I and II are summarized in Section II of this report. These results are used in the formulation of the initial flaw assumptions developed in Task VII as part of the damage tolerant design criteria for attachment lugs.

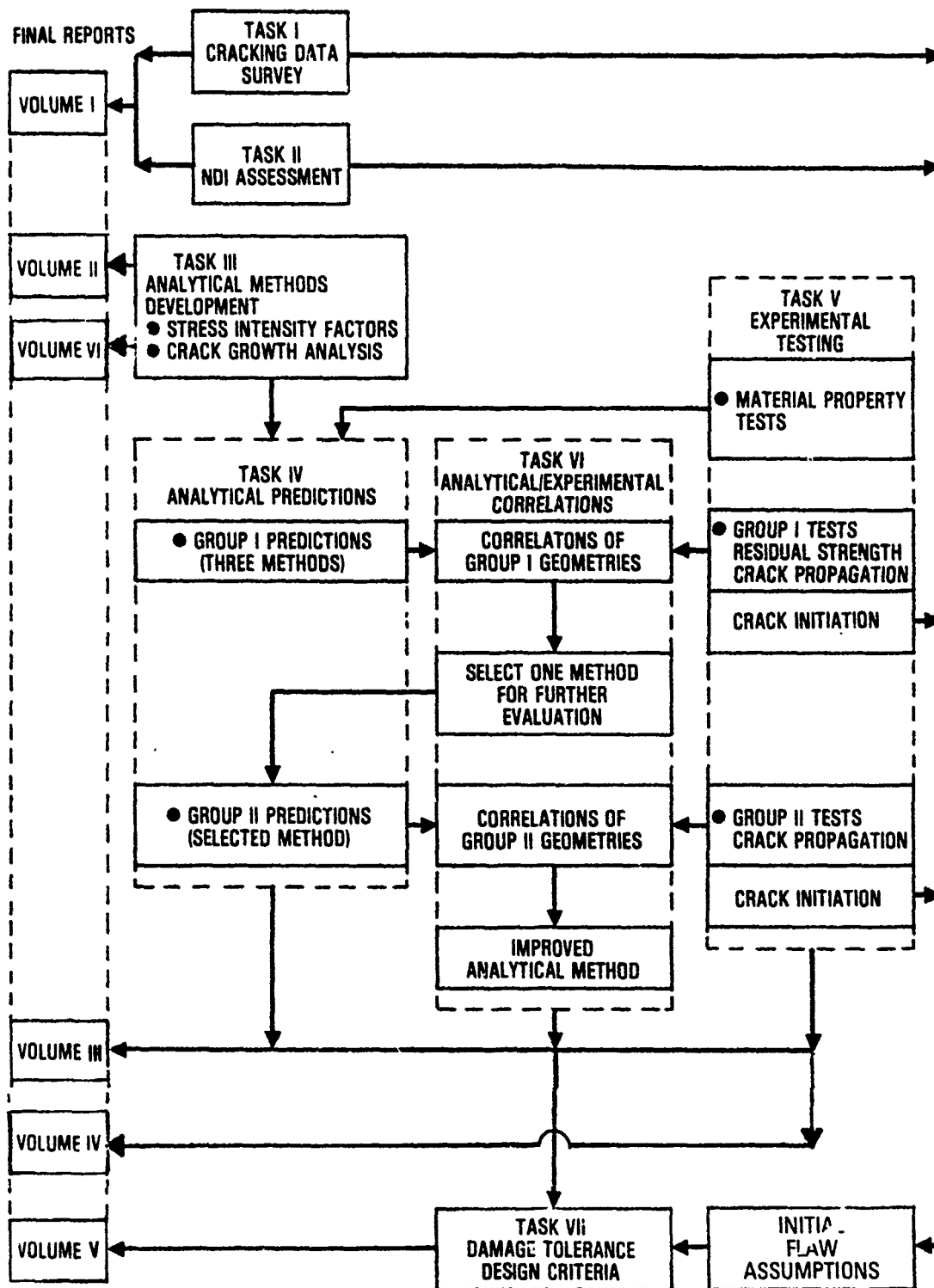


Figure 1-1. Roadmap of the Program

Task III involved the development of three different levels of complexity and degrees of sophistication for determining stress intensity factors for single corner cracks and single through-the-thickness cracks in aircraft attachment lugs, and the development of crack growth analyses capable of predicting the growth behavior of these cracks and the residual strength of these lugs. This work is summarized in Section III.

The methodology developed in Task III was used in Task IV to predict the residual strength and the crack growth behavior for a number of different geometries and test conditions defined in the experimental program. These predictions were made prior to testing. Two groups of attachment lug geometries were tested in Task V. The correlations of test results and analytical predictions constituted Task VI. The analytical methods developed in Task III were evaluated, by correlating the analytical predictions made in Task IV with the Group I experimental test data, and a single method was selected for use in prediction of Group II tests. Further evaluation of the selected method was made by correlating the analytical predictions for the Group II tests (Task IV) with the experimental test results (Task V). The experimental results and comparisons with analysis are presented in Section IV.

Damage tolerant design criteria for aircraft attachment lugs were developed in Task VII. These criteria are similar in nature to those of Military Specification MIL-A-83444, (Reference [6]) and require crack growth analyses by the types of methods developed and verified in Tasks III through VI. The recommended criteria are presented in Section V.

As Figure 1-1 shows, the following sequence of final report volumes is generated to cover the work conducted under this project:

- Volume I. Cracking Data Survey and NDI Assessment for Attachment Lugs
- Volume II. Crack Growth Analysis Methods for Attachment Lugs
- Volume III. Experimental Evaluation of Crack Growth Analysis Methods for Attachment Lugs
- Volume IV. Tabulated Test Data for Attachment Lugs

Volume V. Executive Summary and Damage Tolerance Criteria
Recommendations for Attachment Lugs

Volume VI. User's Manual for "LUGRO" Computer Program to Predict Crack
Growth in Lugs

SECTION II

SERVICE CRACKING SURVEY AND NDI ASSESSMENT

The cracking data survey and NDI evaluation [1] were carried out to examine the origin causes of cracking in attachment lugs, the causes of failure, the initial crack type, shape, and location, the likelihood of multiple cracking, the critical crack size, and to estimate inspectable flaw sizes for lugs.

1. CAUSES OF SERVICE CRACKING AND SERVICE FAILURES

Corrosion/stress corrosion and fatigue/fretting are the two major causes of initial cracking in aircraft lugs in service. Only 8 of the 160 service failures surveyed (5 percent) were traced to initial defects.

As Figure 2-1 shows, fatigue crack growth and stress corrosion cracking are also the two leading causes of service failures in lugs. Static overload is the third major cause. These results vary somewhat with material. In aluminum lugs in service, fatigue/fretting and corrosion/stress corrosion are about equally likely causes, both for crack initiation and crack growth. In steel lugs, however, corrosion/stress corrosion is the more frequent cause by a ratio of more than two to one.

In the service data survey, the 55 failures resulting from fatigue crack growth were given special attention; Figure 2-2. Of these, 42 of the cracks (76 percent) initiated by fatigue/fretting and only six (11 percent) from initial defects.

2. CRACK TYPE, SHAPE AND LOCATION

The common initial crack types for lugs in service are surface cracks in the bore of the hole, corner cracks, and surface cracks on the lug face near the hole, in that order.

The presence of a bushing or bearing tends to affect the type of initial crack. Surface cracks in the bore of the hole occur more frequently and surface cracks on the lug face less frequently in lugs with

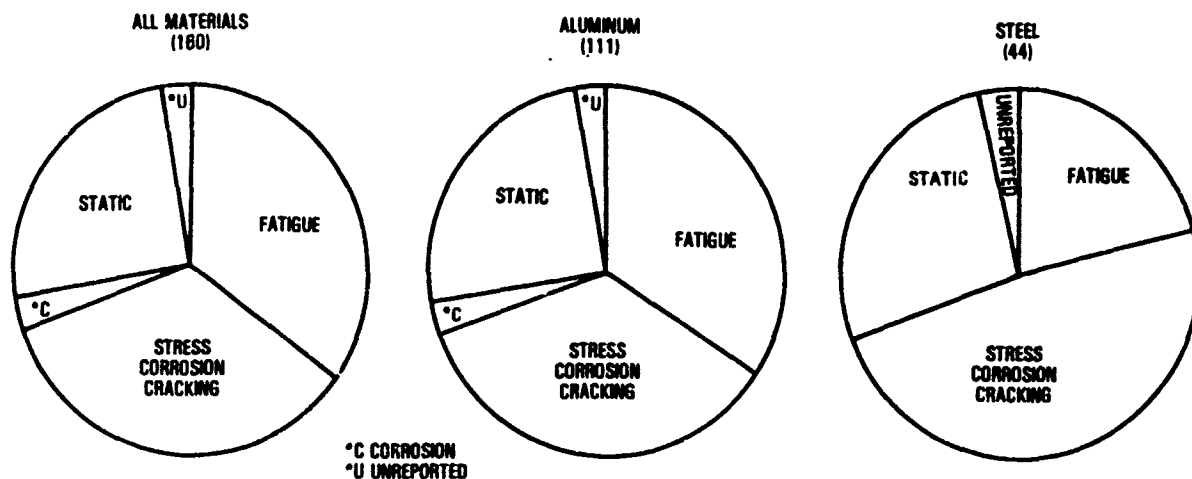


Figure 2-1. Causes of Failure for Lugs in Service

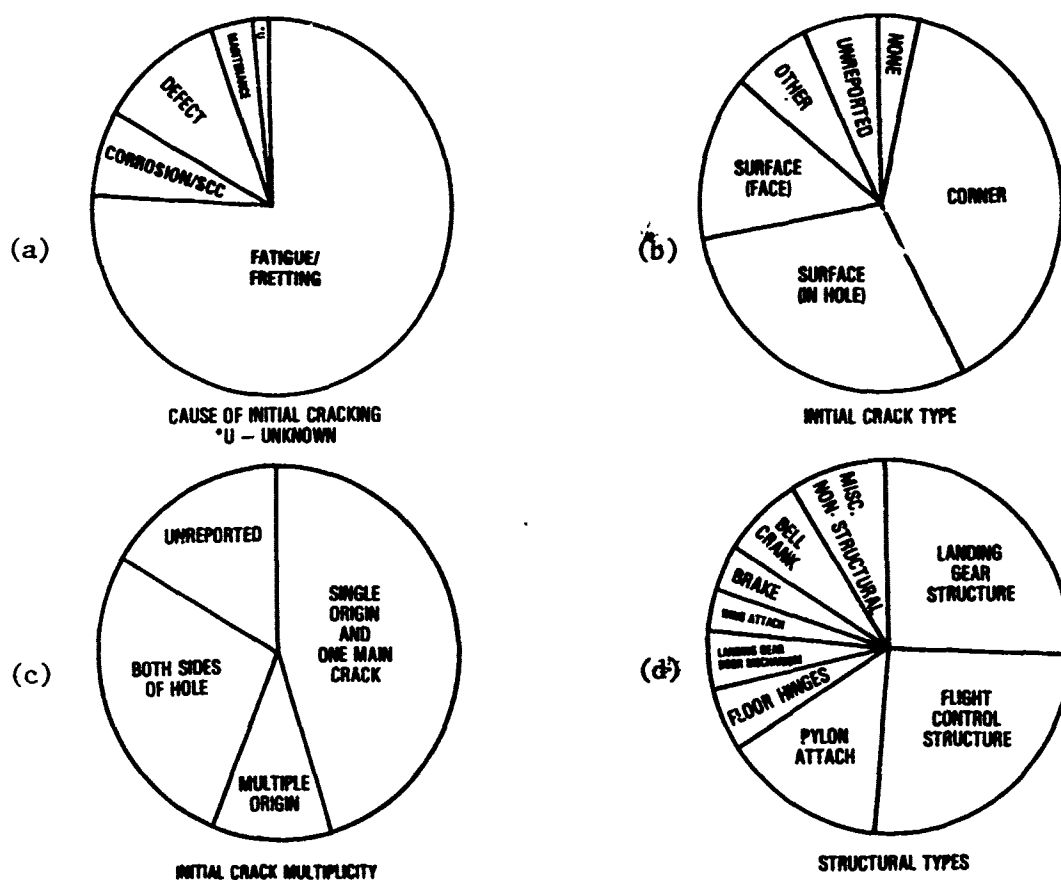


Figure 2-2. Results for 55 Lugs that Failed in Service by Fatigue Crack Growth

bushings or bearings; the reverse was true in lugs without bushings or bearings.

Corner cracks were the most common initial crack type in the 55 service failure cases which failed in fatigue, occurring 38 percent of the time; Figure 2-2(b). Corner cracks were also the most common initial crack type in full-scale fatigue tests of lugs. This is in contrast to the cases which failed by stress corrosion, where only 12 percent were corner cracks compared to 47 percent surface cracks in the hole bore.

The predominant shape of corner cracks in lugs can be estimated from lug coupon fatigue data. Coupon data from the literature indicated that the ratio of depth "a" to radial length "c" of a corner crack in a lug without out-of-plane bending tends to be about 1.3 or greater.

Criteria for crack location can be evaluated using lug coupon fatigue data. Based on data reviewed in [1], crack location seemed to coincide with either the maximum tangential stress location or the location of the edge of the zone of contact with the pin. These locations can be calculated by finite element analyses, and depend on load direction, fit of the pin or bushing, and to a lesser extent load magnitude.

3. CRACK MULTIPLICITY

Multiple-origin cracks and cracks on both sides of the lug hole are common in lug fatigue coupons which have no preflaws and no compressive residual stresses. In the 55 service fatigue failure cases surveyed, multiple-origin cracks and cracking on both sides of the hole occurred almost as frequently as single-origin cracking, Figure 2-2(c). Full-scale fatigue test results for 24 lugs show the same trend with respect to flaw multiplicity.

When multiple crack origins along the hole bore coalesce they tend to form a through-thickness crack at a relatively short radial length.

4. CRITICAL AND INSPECTABLE CRACK SIZES

The critical crack size reported for 35 service fatigue failures of lugs in Air Force aircraft structure are summarized in Figure 2-3. The

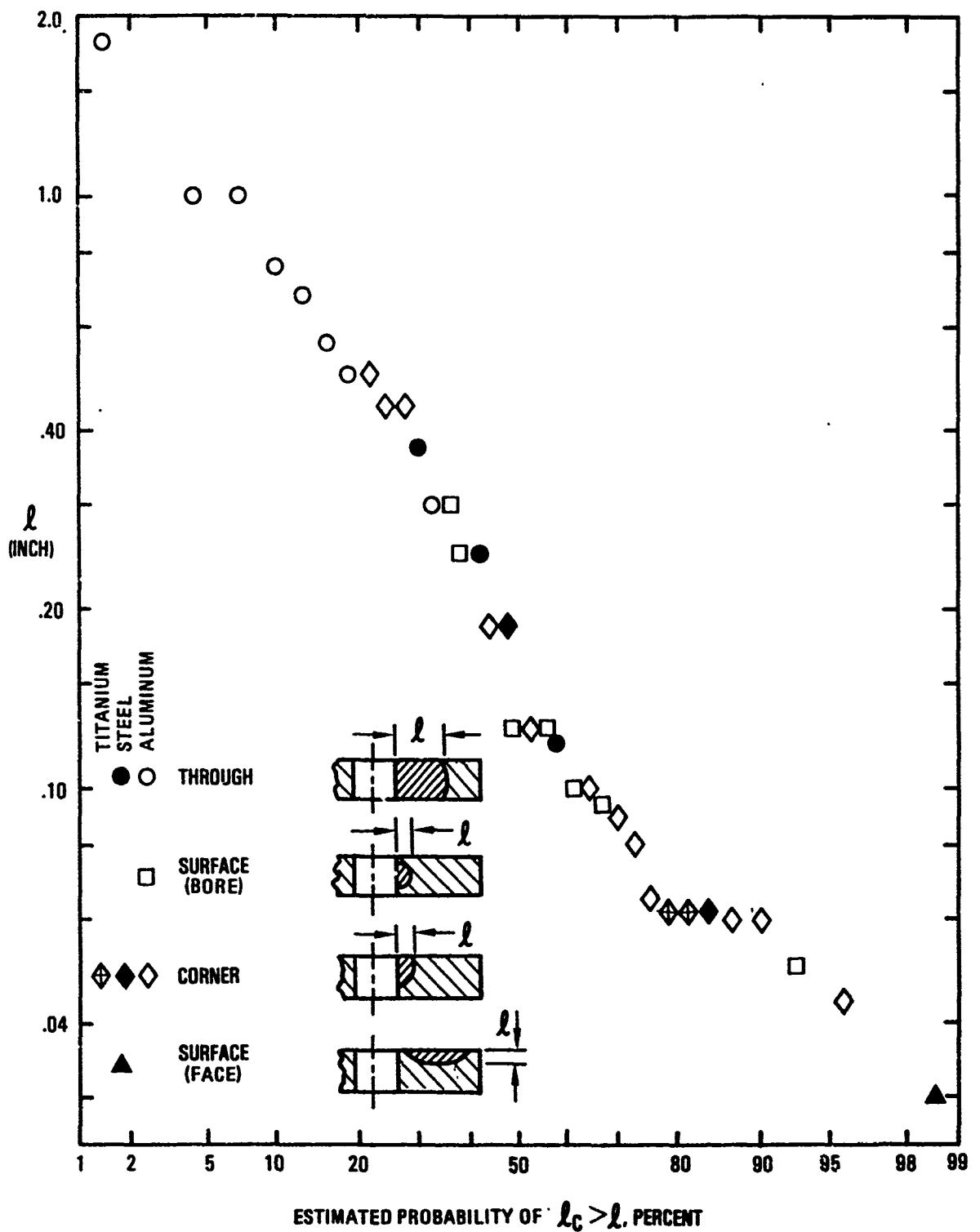


Figure 2-3. Critical Crack Sizes After Fatigue Crack Growth in 35 Service Failed Lugs (Air Force ALC Data Only)

median critical crack size was 0.125 inch radial length. Twenty-five percent of the critical crack sizes were under 0.070 inch radial length.

These small critical crack sizes in lugs seem to suggest that required initial flaw sizes for damage tolerance design of lugs must also be small; otherwise these requirements can be too costly on lug design.

The problem of establishing reliably detectable initial flaw sizes for lugs is a statistical problem requiring inspection data. However, statistical NDI data on lugs are not available to establish the detectable flaw size for a required detection probability and confidence level. Therefore, an inspectable flaw size can only be proposed or hypothesized, subject to verification.

A corner crack, or surface crack at the hole bore, 0.025 inch in radial length appears feasible for manufacturing inspection and possibly for inspection at time of overhaul of the lug using selected methods, special steps to improve inspector reliability, and perhaps multiple inspections. A thorough NDI verification program would be needed to substantiate that this flaw size can be detected with 90 percent reliability and 95 percent confidence.

However, the question remains whether inspectability alone can be used as the basis for initial flaw sizes. As mentioned above, only a small percentage of the lug service failures surveyed in Task I were traced to undiscovered initial defects. The balance of the failures would have been unaffected by improved flaw detection practices. Presupposing that an aim of new damage tolerance design requirements for lugs will be to prevent a significant percentage of the type of failures in the survey, other aspects than inspectability must be addressed as well in the process of creating those requirements. This observation leads to continued discussion in Section V of this report.

SECTION III

CRACK GROWTH ANALYSIS METHODS

Analytical methods have been presented in [2] to predict both fatigue crack growth and residual strength of cracked attachment lugs. Crack growth analysis includes the following elements:

- o Stress intensity factor solution
- o Baseline crack growth rate relationship
- o Applied load sequence
- o Spectrum load interaction model

As summarized below, the emphasis in [2] was upon the calculation of stress intensity factors, with only a brief discussion of the alternative constant amplitude fatigue crack growth rate relationships and spectrum load interaction models.

1. STRESS INTENSITY FACTORS FOR STRAIGHT LUGS

Several alternative methods were presented in [2] for the calculation of stress intensity factors for straight attachment lugs subjected to axial loading. These methods include the simple compounding, two-dimensional cracked finite element, weighting function, and three-dimensional cracked finite element method. Parameters and complexities covered in the stress intensity factor solutions presented for straight lugs are outer-to-inner radius ratio (1.50 to 3.0), crack geometry (single corner crack, through-the-thickness crack, and the intermediate transition), crack length (measured on lug face and along bore of hole), change in distribution of pin bearing pressure due to crack length change, ratio of pin modulus to lug modulus (1.0 or 3.0), interference-fit bushings, and elastoplastic analysis when the peak stress at the hole exceeds the material tensile yield strength.

A two-dimensional finite element analysis was used to compute the stress distribution in an uncracked lug. The calculated stress distribu-

tions along the potential crack path are given in Table 3-1 for lugs of various R_0/R_1 ratios.

The compounding method combines known solutions to obtain an engineering approximation for the stress intensity factor. The approximation is given by

$$K_{LUG} = \frac{1}{2} (K_{41} + K_{44}) \quad (3-1)$$

Equations for K_{41} and K_{44} are given in Appendix A of [2].

The two-dimensional cracked finite element method properly models the crack tip stress singularity and the distribution of pin bearing pressure, which changes drastically with crack length. The stress intensity factors calculated by this method are listed in Table 3-2.

The weighting function method calculates the stress intensity factor as the integral of the product of the stress in the uncracked lug times the Green's function for the lug:

$$K_I = \sqrt{\pi c} \int_0^1 G(c, x/c) \sigma(x) d(x/c) \quad (3-2)$$

The Green's functions for straight lugs were developed using two-dimensional cracked finite element analyses with point loads applied on the crack surface. However, these "original" Green's functions, when used with the stress distribution in the uncracked lug from Table 3-1, obtain K_I results at variance with those of the two-dimensional cracked finite element analysis. The discrepancy arises because the Green's function method fails to account for the change in the distribution of pin bearing pressure as the crack grows. To correct the discrepancy, the original Green's functions were modified such that the cracked finite element results are exactly duplicated when these modified Green's functions are used. The original and modified Green's functions are listed in Tables 3-4 through 3-9 of [2].

Figure 3-1 compares the stress intensity factors for through-the-thickness cracks computed by the various methods. Reasonable agreement among all methods is obtained at R_0/R_1 ratios of 2.25 and 3.0, but not at

TABLE 3-1. NORMALIZED UNFLAWED STRESS DISTRIBUTION ALONG x-AXIS FOR STRAIGHT ATTACHMENT LUGS

		σ_y/σ_{br}					σ_y/σ_o				
		1.50	2.00	2.25	2.50	3.00	1.50	2.00	2.25	2.50	3.00
$\frac{x-R_1}{R_o-R_1}$	R_o/R_1										
0.00*		4.389	2.737	2.364	2.100	1.715	6.584	5.474	5.319	5.250	5.145
0.05		3.903	2.313	1.884	1.739	1.367	5.855	4.626	4.239	4.348	4.101
0.15		3.219	1.728	1.375	1.167	0.878	4.829	3.456	3.094	2.918	2.634
0.25		2.677	1.333	1.044	0.842	0.618	4.016	2.666	2.349	2.105	1.854
0.35		2.319	1.105	0.862	0.692	0.499	3.479	2.210	1.940	1.730	1.497
0.45		1.990	0.925	0.723	0.578	0.416	2.985	1.850	1.627	1.445	1.248
0.55		1.736	0.788	0.620	0.493	0.355	2.604	1.576	1.395	1.235	1.065
0.65		1.464	0.651	0.520	0.410	0.299	2.196	1.302	1.170	1.025	0.897
0.75		1.218	0.529	0.432	0.334	0.248	1.827	1.058	0.972	0.835	0.744
0.85		0.894	0.376	0.320	0.242	0.186	1.341	0.752	0.720	0.605	0.558
0.95		0.487	0.213	0.181	0.147	0.111	0.731	0.426	0.407	0.368	0.333

*Extrapolated Values

TABLE 3-2. NORMALIZED STRESS INTENSITY FACTORS FOR SINGLE THROUGH-THE-THICKNESS CRACKS IN STRAIGHT ATTACHMENT LUGS USING CRACKED FINITE ELEMENT METHOD

$\frac{R_o/R_i}{c/(R_o-R_i)}$		$K/(\sigma_{br} \sqrt{\pi c})$					$K/(\sigma_o \sqrt{\pi c})$				
		1.50	2.00	2.25	2.50	3.00	1.50	2.00	2.25	2.50	3.00
0.0		4.916	3.066	2.648	2.352	1.921	7.374	6.131	5.957	5.880	5.762
0.1		3.580	2.237	1.733	1.524	1.153	5.370	4.474	3.899	3.809	3.460
0.2		3.110	1.789	1.389	1.185	0.869	4.665	3.578	3.126	2.963	2.607
0.3		2.945	1.639	1.246	1.060	0.749	4.423	3.277	2.804	2.650	2.246
0.4		2.816	1.506	1.111	0.954	0.657	4.224	3.012	2.500	2.385	1.971
0.5		2.820	1.472	1.076	0.917	0.624	4.230	2.943	2.422	2.293	1.872
0.6		2.824	1.442	1.051	0.892	0.603	4.236	2.884	2.364	2.230	1.810
0.7		2.981	1.509	1.095	0.922	0.620	4.472	3.017	2.463	2.306	1.860
0.8		3.219	1.619	1.176	0.985	0.659	4.828	3.238	2.646	2.463	1.977
0.9		4.080	2.044	1.470	1.246	0.812	6.120	4.088	3.308	3.115	2.436

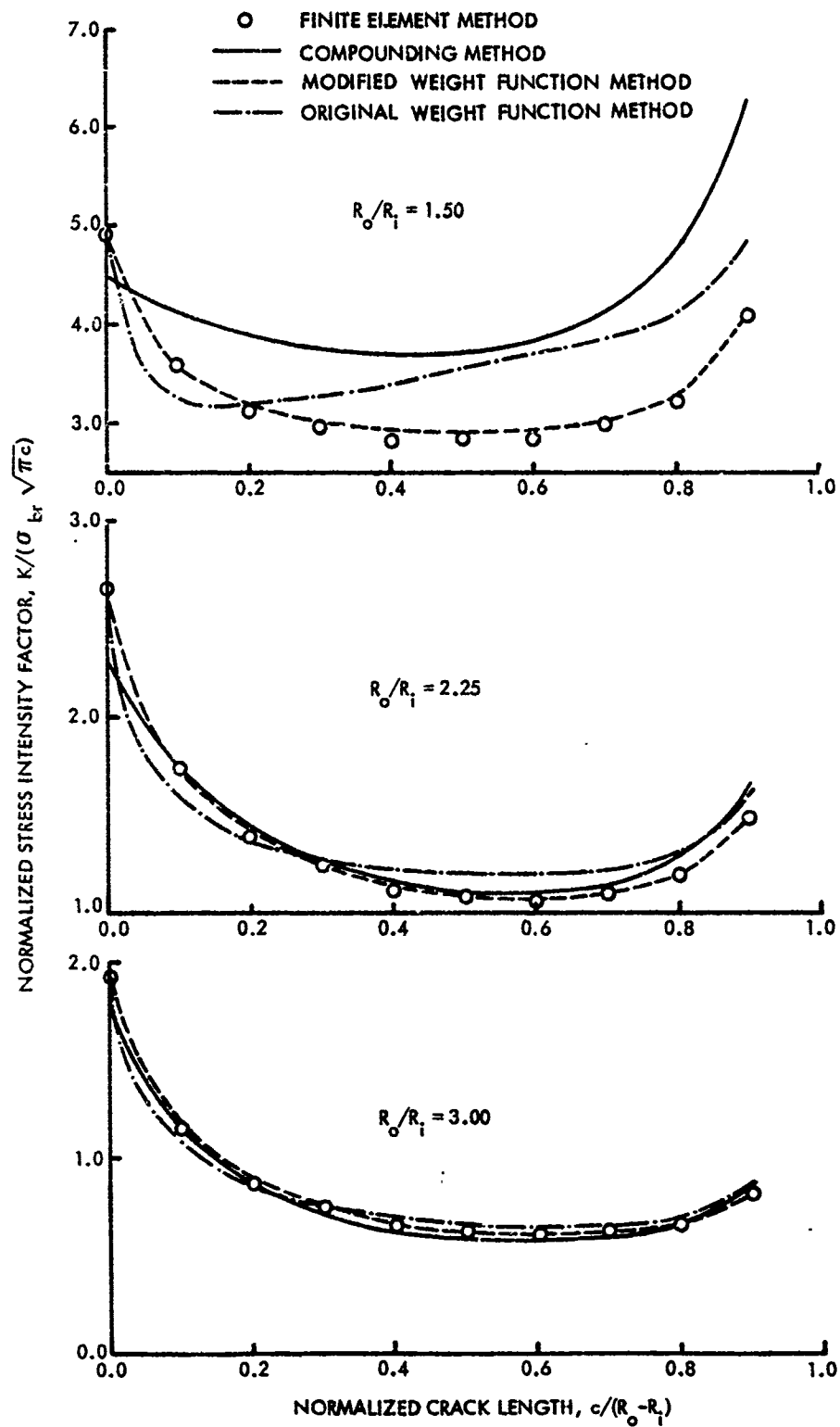


Figure 3-1. Comparison of Stress Intensity Factors Computed Using the Compounding, Weight Function and Cracked Finite Element Methods

$R_o/R_i = 1.50$. Thus, any method could be used for larger R_o/R_i ratios, but the more rigorous two-dimensional cracked finite element method (or equivalently, the Modified Green's function method) is preferred when $R_o/R_i < 2.0$.

The weighting function method can be applied to account for residual stresses caused by a shrink-fit bushing. Assuming the lug and bushing remain in intimate contact during loading, the stress intensity factor is calculated by Equation (3-2) where stress $\sigma(x)$ is the sum of the residual stress caused by bushing installation plus the distribution of stress caused by the applied load. The residual stress is estimated from the closed-form solution for two concentric cylinders. The applied stress is obtained from two-dimensional finite element analysis of an uncracked lug in intimate contact with a neat-fit bushing. If the bushing and lug are of the same material, then the applied stress distribution can be obtained from Table 3-1. This method can give unconservative results when separation occurs between the bushing and lug. An improved method which considers separation is presented in [3] and summarized later in this section.

The solution methods for through-the-thickness cracks can be modified to analyze a corner crack, utilizing a corner crack correction factor, along with a way to account for the transitional behavior as the corner crack becomes a through-the-thickness crack. Two alternative correction factor approaches were suggested in [2], a one-parameter and a two-parameter method.

In the one-parameter method, the flaw shape is assumed to be constant (e.g., $a/c = 1.33$), and the stress intensity factor at the lug surface point (Point C) is calculated by multiplying the stress intensity factor for a through-the-thickness crack by the following factor:

$$\phi_{71}^{(C)} = 1 - \frac{.2886}{1 + 2 \left[\frac{a}{c} \right]^2 \left[\frac{c}{B} \right]^2} \quad (3-3)$$

This equation applies to the crack throughout its growth from corner crack, through transition, to a through-the-thickness crack.

In the two-parameter method, the equations shown in Figure 3-2 are

used to compute stress intensity factors at the lug surface and hole wall (Points C and A). The method used during the transition to a through-the-thickness crack is based on the approach proposed by Collipriest and Ehret [7].

A three-dimensional cracked finite element method, although too expensive for general application, was used to compare the corner crack stress intensity factors generated by the compounding and Green's function methods. The comparison is shown in Figure 3-3 in terms of values of corner crack correction factors at the lug surface by all the three methods.

An elastoplastic analysis was developed for use when the peak stress in the uncracked lug exceeds the material tensile yield strength. An iterative finite element analysis with incremental loading and unloading is used to calculate the stress distributions in the uncracked lug for the maximum and minimum loads of the fatigue cycle. These stress distributions are used with the modified Green's function to estimate K_{\max} and K_{\min} for a lug with a through-the-thickness crack. This nonlinear method is inexact, because strictly speaking the validity of the Green's function method requires linearity between load and stress.

2. STRESS INTENSITY FACTORS FOR TAPERED LUGS

Finite element analyses were employed [2] to obtain stress intensity factors for tapered attachment lugs subjected to either axial or off-axis loading. Only unbushed lugs with a 45-degree taper angle were analyzed.

A two-dimensional finite element analysis was used to calculate the critical locations for cracking and the stress distribution in an uncracked lug. For axial as well as off-axis loading, there are two angular locations of peak tangential stresses. Figure 3-4 shows these two angular locations for different R_o/R_i ratio values, where 1 and 2 correspond to most severe and less severe peak tangential stress locations, respectively. For axial loading, stresses along the critical 90-degree line are listed in

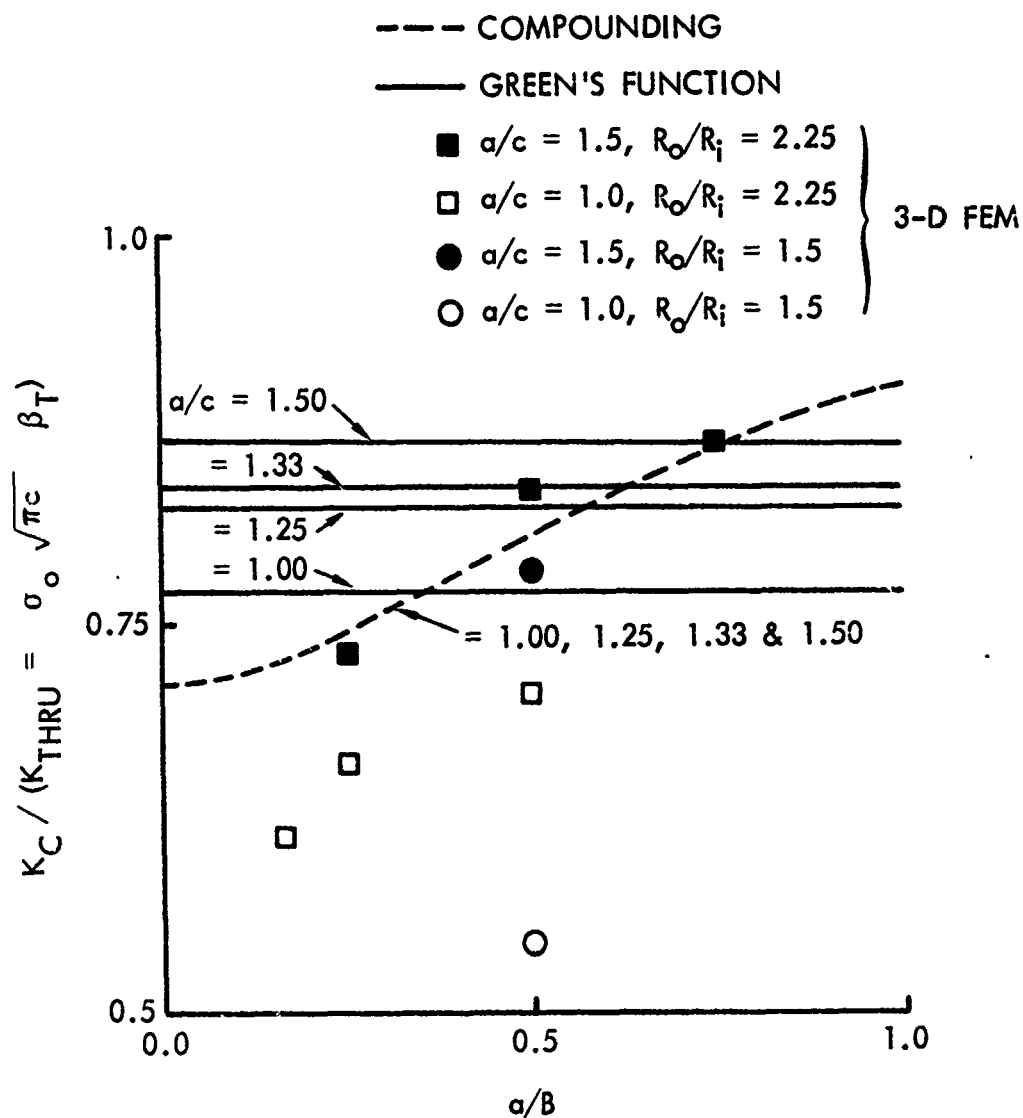


Figure 3-3. Comparison of Corner Crack Correction Factors at the Lug Surface by the Three Methods

SYMBOL	LOAD DIRECTION
--○--	0°
—△—	-45°
—□—	-90°

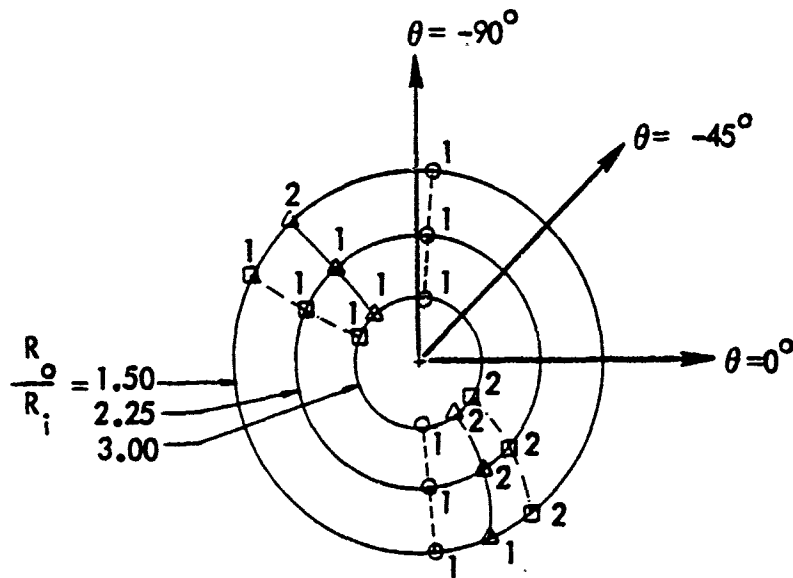


Figure 3-4. Fatigue Critical Locations of Tapered Lugs Subjected to Various Load Orientations

Table 3-3 for five values of R_o/R_i , and Equation 3-4 is an equation for bearing stress concentration factor for axial loading of a tapered lug with a taper angle, β , between 45 degrees and 0 degrees (i.e., straight lug):

$$K_{tb} = \frac{\sigma_{max}}{\sigma_{br}} = (2.75 - \frac{\beta^0}{135}) (\frac{R_o}{R_i} - 1) - (0.675 - \frac{\beta^0}{1000}) \quad (3-4)$$

Stress intensity factor results obtained using the cracked element are listed in Table 3-4 for axial tension loading of 45-degree tapered lugs having R_o/R_i ratios from 1.5 to 3.0. Off-axis loading solutions for stress intensity factor are plotted in Figures 3-5 and 3-6 for a tapered lug with $R_o/R_i = 2.25$, loaded in the -45 and -90 degree directions, with a crack at either of the two most critical orientations.

For corner cracks in tapered lugs, either corner crack correction factor can be used in conjunction with the appropriate through-the-thickness stress intensity factors. For problems involving bushings or stresses above the material yield strength, the weighting function methods would be applicable, but now Green's functions would be needed for tapered lugs and for each new loading direction and crack orientation. As an approximation, the Green's function for the axially-loaded straight lug with the same R_o/R_i ratio may be used, although the accuracy of this approximation is questionable, particularly for off-axis loading.

3. FATIGUE CRACK GROWTH COMPUTATION

An automated computer program has been developed using state-of-the-art methodologies for prediction of residual strength and fatigue crack growth behaviors of single through-the-thickness cracks and single corner cracks at attachment lugs. This crack growth analysis program is described, and user's instructions are presented, in [5]. The program includes the following four elements:

- o Stress intensity factor solution
- o Baseline crack growth rate relationship

TABLE 3-3. NORMALIZED UNFLAWED STRESS DISTRIBUTION ALONG x-AXIS FOR TAPERED ATTACHMENT LUGS

$\frac{(x-R_1)}{(R_0-R_1)}$	R_0/R_1	σ_y/σ_{br}						σ_y/σ_0					
		1.50	2.00	2.25	2.50	3.00		1.50	2.00	2.25	2.50	3.00	
0.00*		3.768	2.405	2.104	1.878	1.562		5.652	4.810	4.734	4.695	4.686	
0.05		3.393	2.109	1.783	1.593	1.260		5.090	4.218	4.012	3.981	3.780	
0.15		2.770	1.540	1.292	1.057	0.799		4.155	3.080	2.907	2.643	2.397	
0.25		2.320	1.190	0.945	0.762	0.563		3.480	2.380	2.126	1.905	1.689	
0.35		2.034	0.998	0.793	0.632	0.458		3.051	1.996	1.784	1.580	1.374	
0.45		1.778	0.854	0.681	0.538	0.388		2.667	1.708	1.532	1.345	1.164	
0.55		1.588	0.747	0.592	0.470	0.339		2.382	1.494	1.332	1.175	1.017	
0.65		1.396	0.647	0.521	0.408	0.297		2.094	1.294	1.172	1.020	0.891	
0.75		1.246	0.564	0.452	0.355	0.263		1.869	1.128	1.017	0.888	0.789	
0.85		1.080	0.475	0.391	0.298	0.230		1.620	0.950	0.880	0.745	0.690	
0.95		0.882	0.408	0.332	0.252	0.209		1.323	0.816	0.747	0.630	0.627	

*Extrapolated Values

TABLE 3-4. NORMALIZED STRESS INTENSITY FACTORS FOR SINGLE THROUGH-THICKNESS
CRACKS IN TAPERED ATTACHMENT LUGS USING CRACKED FINITE ELEMENT METHOD

$\frac{R_o/R_1}{\frac{c}{(R_o-R_1)}}$	$K/(\sigma_{br} \sqrt{\pi c})$						$K/(\sigma_o \sqrt{\pi c})$					
	1.50	2.00	2.25	2.50	3.00	1.50	2.00	2.25	2.50	3.00	1.50	2.00
0.0	4.220	2.694	2.356	2.103	1.749	6.330	5.388	5.301	5.258	5.247		
0.1	3.319	1.968	1.588	1.409	1.078	4.979	3.936	3.573	3.523	3.234		
0.2	2.867	1.556	1.255	1.052	0.799	4.301	3.112	2.824	2.630	2.397		
0.3	2,672	1.408	1.115	0.928	0.685	4.008	2.816	2.509	2.320	2.055		
0.4	2.500	1.276	0.988	0.827	0.602	3.750	2.552	2.223	2.068	1.806		
0.5	2.433	1.224	0.943	0.782	0.564	3.650	2.448	2.122	1.955	1.692		
0.6	2.363	1.173	0.903	0.745	0.535	3.545	2.346	2.032	1.863	1.605		
0.7	2.386	1.179	0.912	0.745	0.534	3.579	2.358	2.052	1.863	1.602		
0.8	2.410	1.188	0.932	0.746	0.545	3.615	2.376	2.097	1.865	1.635		
0.9	2.479	1.273	1.017	0.794	0.585	3.719	2.546	2.288	1.985	1.755		

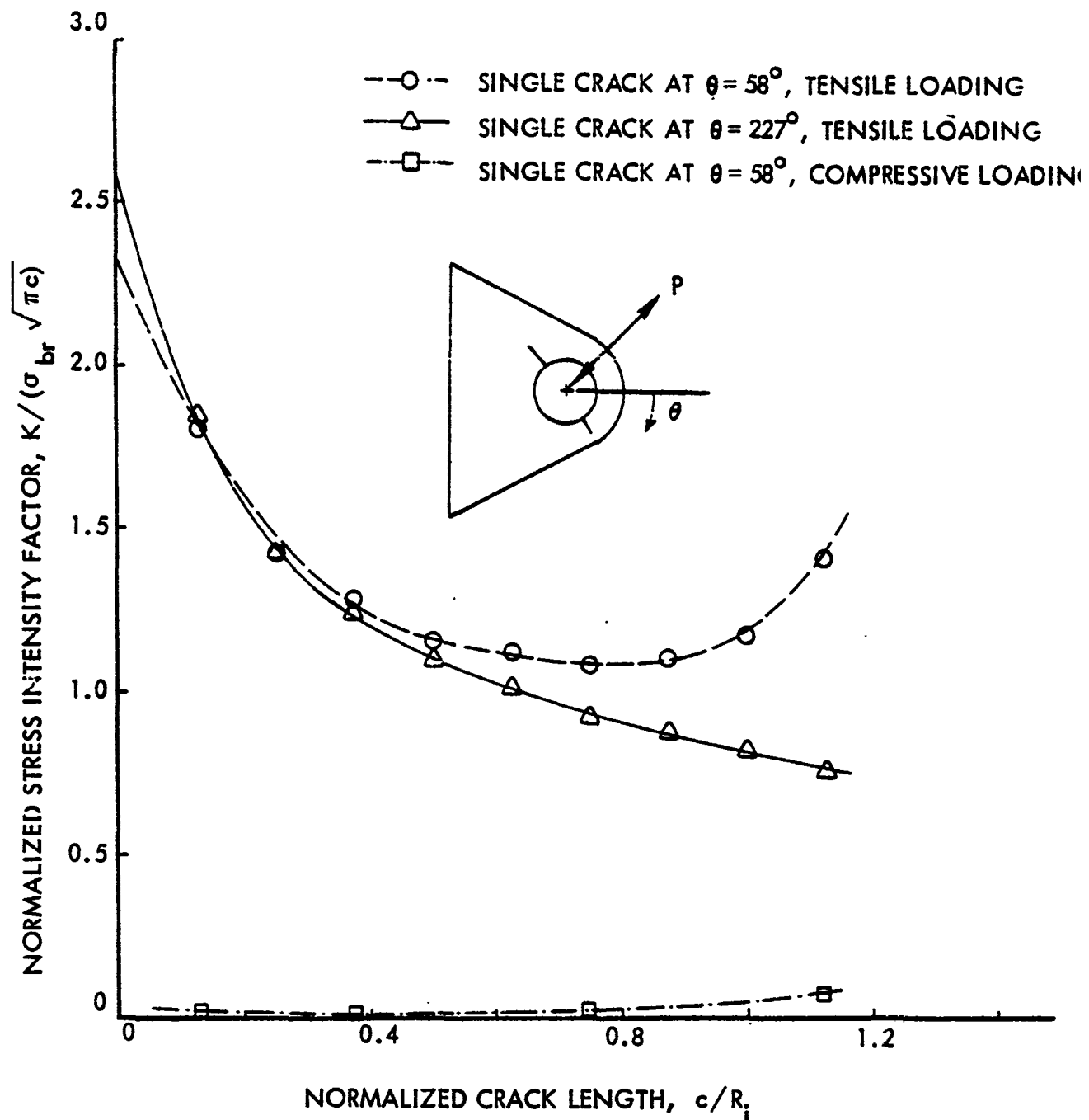


Figure 3-5. Normalized Stress Intensity Factors for Single Through-the-Thickness Cracks Emanating from a Tapered Lug Subjected to a Pin Loading Applied in -45° and its Reversed Directions ($R_o/R_i = 2.25$)

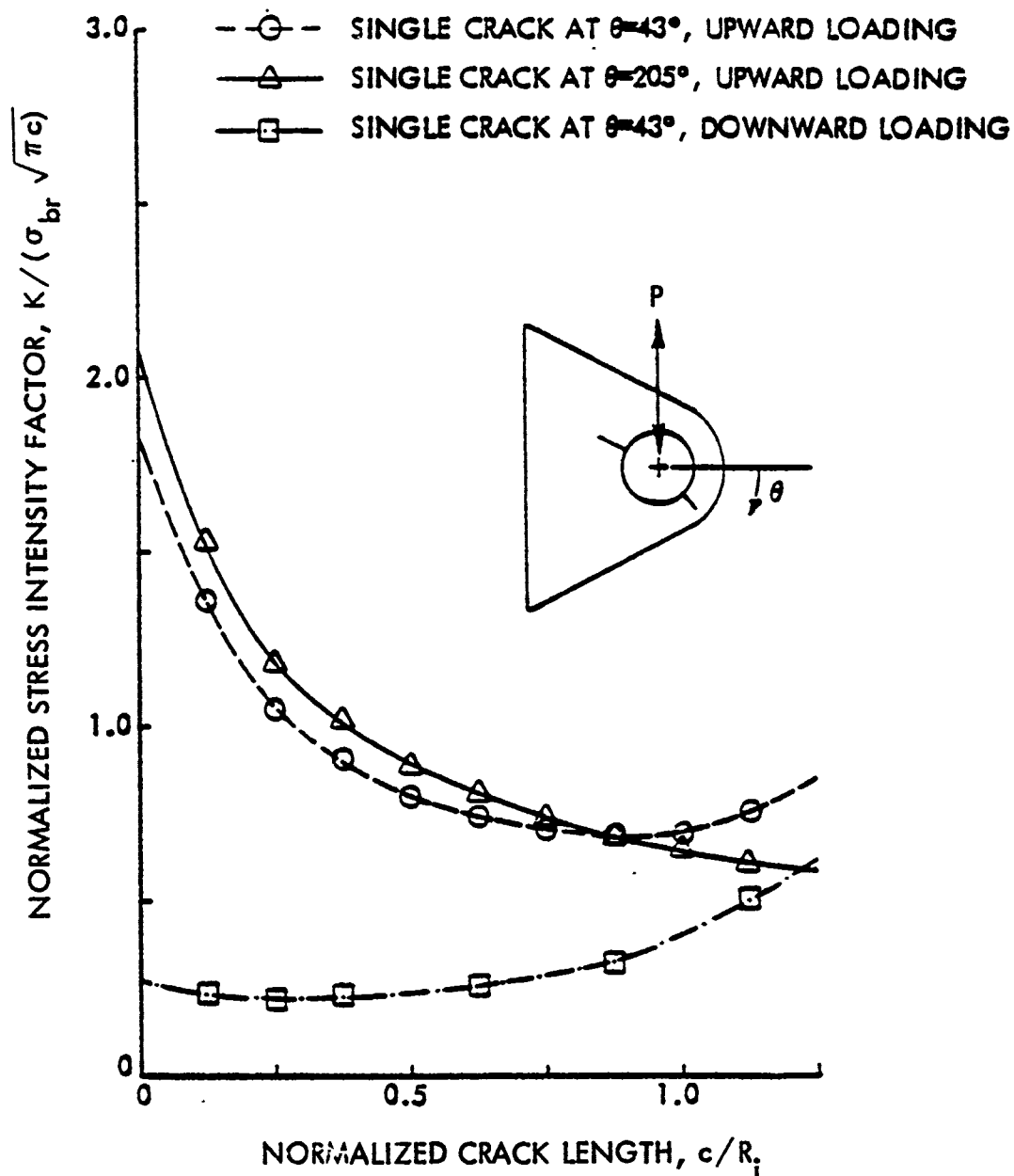


Figure 3-6. Normalized Stress Intensity Factors for Single Through-the-Thickness Cracks Emanating from a Tapered Lug Subjected to a Pin Loading Applied in -90° and its Reversed Directions ($R_o/R_i = 2.25$)

- o Applied load sequence
- o Spectrum load-interaction model.

Stress intensity factor solutions for attachment lugs developed under this contract for a variety of structural and loading complexities are given in [2] and are incorporated in the program.

The optional baseline crack growth rate relationships embedded in the program are those of Paris, Forman, and Walker. The optional spectrum load-interaction models incorporated in the program are: the Wheeler, Willenborg, Generalized Willenborg, and Hsu models, or assuming no load interaction. The stress levels which comprise each individual mission segment, and from which a mission mix spectrum can be generated, may be input in five optional ways: as maximum stress (σ_{\max}) and stress ratio (R); σ_{\max} and minimum stress (σ_{\min}); σ_{\max} and mean stress (σ_{mean}); σ_{mean} and alternating stress (σ_{alt}); or R and stress range ($\Delta\sigma$). The program predicts the crack growth using a block-by-block integration technique.

For through-the-thickness cracks, either the compounding solution or the Green's function solution can be used in the prediction. In predicting the growth behavior of a single corner crack, the through-the-thickness crack solution may be modified by either the one-parameter (i.e., constant a/c ratio) or two-parameter method. For one-parameter analysis, the prediction is straightforward and is similar to through-the-thickness crack prediction. For two-parameter analysis, it is assumed that for a given number of applied load cycles, the extension of the quarter elliptical crack border is controlled by the stress intensity factors at the intersection of the crack periphery at the hole wall and the lug surface, i.e., K_A and K_C . In general, the stress intensity factors at these two locations are different, resulting in different crack growth rates. Therefore, the new flaw shape aspect ratio after each crack growth increment will be different from the preceding one. The new crack aspect ratio is computed using the new crack lengths on both the hole wall and lug surface. The process will be repeated until the crack length along the hole wall is equal to the lug thickness. At that time the transitional crack growth criterion is used until the crack has achieved a uniform format. After that, if the failure has not occurred, a one-dimensional through-the-

thickness crack analysis is used to continuously predict the subsequent crack growth life. The analysis is considered to be complete when fracture occurs or when the desired final crack length or the maximum usage time is reached.

4. REVISED ANALYSIS METHODS

Methodology improvements, new finite element solutions, and a new analysis method, developed after the completion of [2], were reported in [3].

Two method improvements were attempted. First, net section yielding was established as an alternative failure criterion for a lug; equations for critical crack size based on net section yielding were presented for several crack configurations. The second was an unsuccessful attempt to improve the compounding method solution presented in [2].

New finite element solutions were obtained for tapered lugs with steel bushings and the simulated wing-pylon attach lug.

Finally, a new analytical method was developed to account for separation between a lug and bushing during loading. First, the finite element model for the wing-pylon lug was revised to model lug-bushing separation with an unknown region of radial contact. Figure 3-7 shows the increase in stresses at a given load, compared to assuming intimate contact between bushing and lug. Used with the Green's function, these increased stresses result in increased values of stress intensity factor, correcting a source of unconservatism in the former analysis method. Secondly, an approximate method was proposed to estimate the stresses by assuming that the bushing and pin act together as a larger pin.

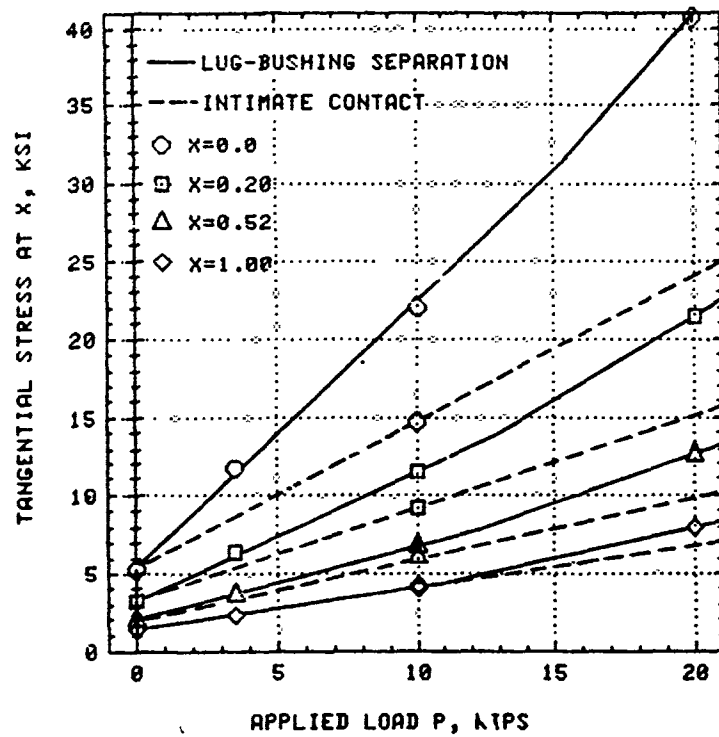


Figure 3-7. Comparison of Calculated Tangential Stress on the Eventual Crack Path in the Simulated Wing-Pylon Lug, Assuming Lug-Bushing Separation or Intimate Contact

SECTION IV

CRACK GROWTH TEST RESULTS AND CORRELATIONS

The results of the damage tolerance predictions, tests, and correlations (Tasks IV, V and VI), as reported in [3], are summarized in this section.

1. EXPERIMENTAL PROGRAM

The main objective of the experimental program was to provide data to evaluate and verify the developed stress intensity factors and crack growth analysis methods and to assist the development of the initial flaw assumptions for the damage tolerance design criteria for aircraft attachment lugs.

The experimental program was first divided into two groups, namely Group I and Group II. The main objectives of the Group I tests were to obtain basic material property data and to generate basic data on lugs to evaluate and verify the analysis methods developed in this program. The main objective of the Group II tests was to evaluate the applicability of these methodologies to more complex situations typical of actual aircraft lug design practices.

The two groups of tests were performed sequentially, Group I first at Lockheed-Georgia Company and Group II second at Lockheed-California Company.

The Group I tests are summarized in Table 4-1 and consisted of a comprehensive study of axially-loaded straight-shank lugs, Figure 4-1(a). A total of 192 lugs (including 16 crack initiation tests) were tested in Group I, as well as 32 material characterization specimens.

Crack growth testing covered two different materials (7075-T651 Aluminum and 4340 Steel), three different outer to inner radius ratios ($R_0/R_1 = 1.50, 2.25$ and 3.0), two different positive stress ratios ($R = 0.1$ on 0.5), two different initial crack geometries (single corner and single through-the-thickness), and two different stress levels (peak notch stress above

TABLE 4-1. SCOPE OF GROUP I RESIDUAL STRENGTH
AND CRACK PROPAGATION TESTS

TYPE OF TEST		R _o / R _i			B (INCH)		TYPE OF LOADING				TYPE OF FLAW		BUSHING		NO. OF TESTS			
		1.5	2.25	3.0	0.25	0.50	STATIC	SPECTRUM		C.A. @ R =		CORNER	THRU	NO		YES		
								BLOCK	F-B-F	0.1	0.5							
BASELINE TESTS	STATIC RESIDUAL STRENGTH	X (8) ⁺				X (8)	X (8)					X (8)		X (8)		8**		
				X (8)		X (8)	X (8)					X (8)	X (8)		8**			
	PROPAGATION	C.A.	ALU	X (16)	X (16)	X (16)		X (48)			X (24)	X (24)	X (24)	X (24)	X (48)		48***	
			STE	X (8)	X (8)	X (8)		X (24)			X (12)	X (12)	X (12)	X (12)	X (24)		24	
		BLOC. SPECTRUM	ALU	X (8)	X (8)	X (8)		X (24)		X (24)			X (12)	X (12)	X (24)		24***	
			STE	X (4)	X (4)	X (4)		X (12)		X (12)			X (6)	X (6)	X (12)		12	
		F-B-F SPECTRUM	STEEL	X (12)	X (12)	X (12)		X (36)		X (36)			X (18)	X (18)	X (36)		36++	
	VARIATIONAL TESTS	C.A. PROPAGATION	0.25 IN. THICKNESS	ALU		X (4)					X (4)		X (4)		X (4)		4***	
				STE		X (2)		X (2)			X (2)		X (2)		X (2)		2	
			BUSHING	ALU		X (4)			X (4)			X (4)			X (4)		X (4)	4***
				STE		X (2)			X (2)			X (2)			X (2)		X (2)	2
F-B-F SPECTRUM		STEEL	0.25 THICK		X (2)		X (2)			X (2)			X (2)		X (2)		2+++	
			BUSHING		X (2)			X (2)			X (2)			X (2)		X (2)	2+++	
		TOTAL		56	64	56	8	168	16	36	40	48	36	88	88	168	8	176

+ NUMBER IN THE PARENTHESIS REPRESENTS NUMBER OF TESTS UNDER PARTICULAR COLUMN

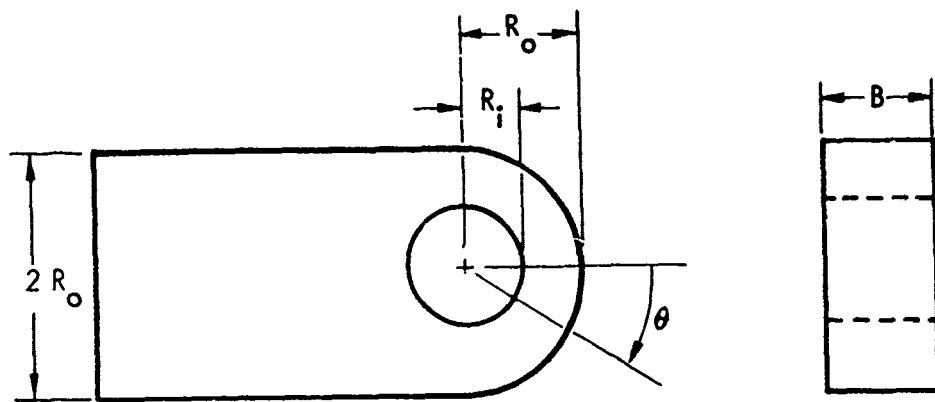
* ALL TESTS ARE DUPLICATED

** TESTS INCLUDE 2 CRACK LENGTHS AND 2 MATERIALS

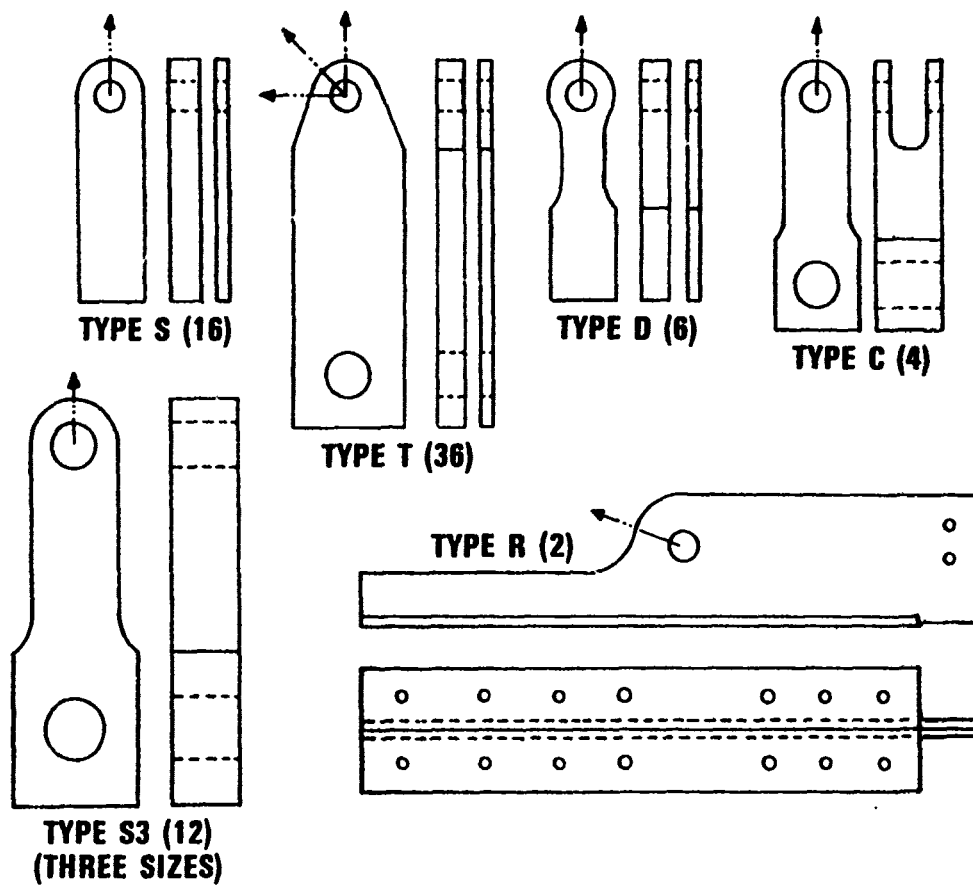
*** TESTS INCLUDE 2 STRESS LEVELS

++ TESTS INCLUDE 3 FLIGHT-BY-FLIGHT SPECTRA (1 CARGO, 1 SEVERE CARGO AND 1 FIGHTER)

+++ SEVERE CARGO SPECTRUM



(a) Group I



(b) Group II

Figure 4-1. Geometries of Group I and Group II Test Specimens

and below yield), in almost a full 3×2^4 test matrix. Additional Group I crack growth testing considered block and flight simulation spectrum loading, lugs with shrink-fit bushings, and thinner lugs ($2R_1/B=6.0$ instead of 3.0). Other Group I tests included fatigue tests of uncracked lugs, residual strength tests of lugs, and material characterization tests.

Group II testing employed the lug geometrics and loading directions sketched in Figure 4-1(b). Seventy-six lugs with corner precracks were fatigue crack growth tested in the four matrices of tests listed in Table 4-2. In addition, there were 8 crack initiation tests of lugs and 11 compact tension crack growth tests for Group II.

Major variables addressed in the Group II tests include nominal diametrical pin clearances of 0.005 inch, 0.0015 inch and 0.0030 inch; pin lubrication (greased or dry); lug shape (straight, tapered, dogbone, clevis); off-axis loading (-45 degrees or -90 degrees to lug axis); initial crack criticality (two angular locations); shrink-fit bushings (bushed or unbushed); and scale-up effects ($2R_1=0.625, 1.0$ or 1.5 in.). Also included in Group II were complex redundant structural lugs, load reversals, and flight simulation spectrum loading. Aluminum was used in 72 of the 84 lugs tested. Finally, in specifying thickness B , outer radius R_o , and inner radius R_i for the Group II specimens, an effort was made to select values of the ratios R_o/R_i , $2R_1/B$, and $(R_o-R_i)/B$ representing the full range for actual aircraft lugs.

2. RESULTS AND CONCLUSIONS FROM GROUP I TESTS

All the aluminum lugs with no preflaws subjected to fatigue crack initiation tests had both primary and secondary flaws and failures. For steel lug crack initiation tests, some specimens did not have any secondary origins. The fatigue threshold of the steel lugs was above 14 ksi, and thus the stress levels were increased to conduct the crack initiation tests.

In residual strength tests, failures of all the corner crack and some through-the-thickness crack specimens, the failures were due to net-section yielding rather than the exceedance of the critical stress intensity values. Accuracy of predicted residual strength is shown in Figure 4-2.

TABLE 4-2. SCOPE OF GROUP II CRACK PROPAGATION TESTS

PIN CLEARANCE, ±.00025 (INCH)		STRAIGHT LUG AXIAL LOADING		TAPERED LUG -45° LOADING LUBRICATED PIN		(a) <u>Pin Clearance and Lubrication and Crack Location</u> Loading: R = 0.1 Thickness: 1.0 inch Material: Aluminum No bushings
		DRY	LUBED	58° CRACK	227° CRACK	
.0005		2	2	2	2	
.0015		2	2	2	2	
.0030		2	2	2	2	

LUG GEOMETRY		B = 1.0 INCH		B = 0.5 INCH		(b) <u>Lug Geometry, Thickness, Bushings</u> Load Direction: Axial Loading: R = 0.1 Material: Aluminum Pin Lubricated
		BUSHING	NO BUSH	BUSHING	NO BUSH	
Straight		2	(2)	2	—	
Tapered		2	2	2	—	
Dogbone		2	2	2	—	
Clevis		—	—	2	2	

LOADING		ALUMINUM B = 1.0 INCH		STEEL B = 0.5 INCH		(c) <u>Loading Direction, Material, Bushings, Reversed Loading</u> Geometry: Tapered Lugs Pin Lubricated
		BUSHING	NO BUSH	BUSHING	NO BUSH	
DIRECTION	R					
0°	0.1	(2)	(2)	—	—	
-45°	0.1	2	(2)	2	2	
-90°	0.1	2	2	2	2	
-90°	-0.5	2	2	—	—	

LUG GEOM.	2R _i (INCH)	R = 0.1	80 FLT SPECTRUM		(d) <u>Size Effect, Thick Lugs, Spectrum Loading, Wing-Pylon Lug</u> Pin Lubricated
		NO BUSH	NO BUSH	BUSHING	
Straight	.625	2	2	—	
2R _i /B = 2/3	1.0	2	2	—	
Axial Load	1.5	2	2	—	
Wing-Pylon 157° Load	1.0	—	—	2	

NOTES: () indicates specimens already included in above submatrix
All specimens contain initial corner cracks

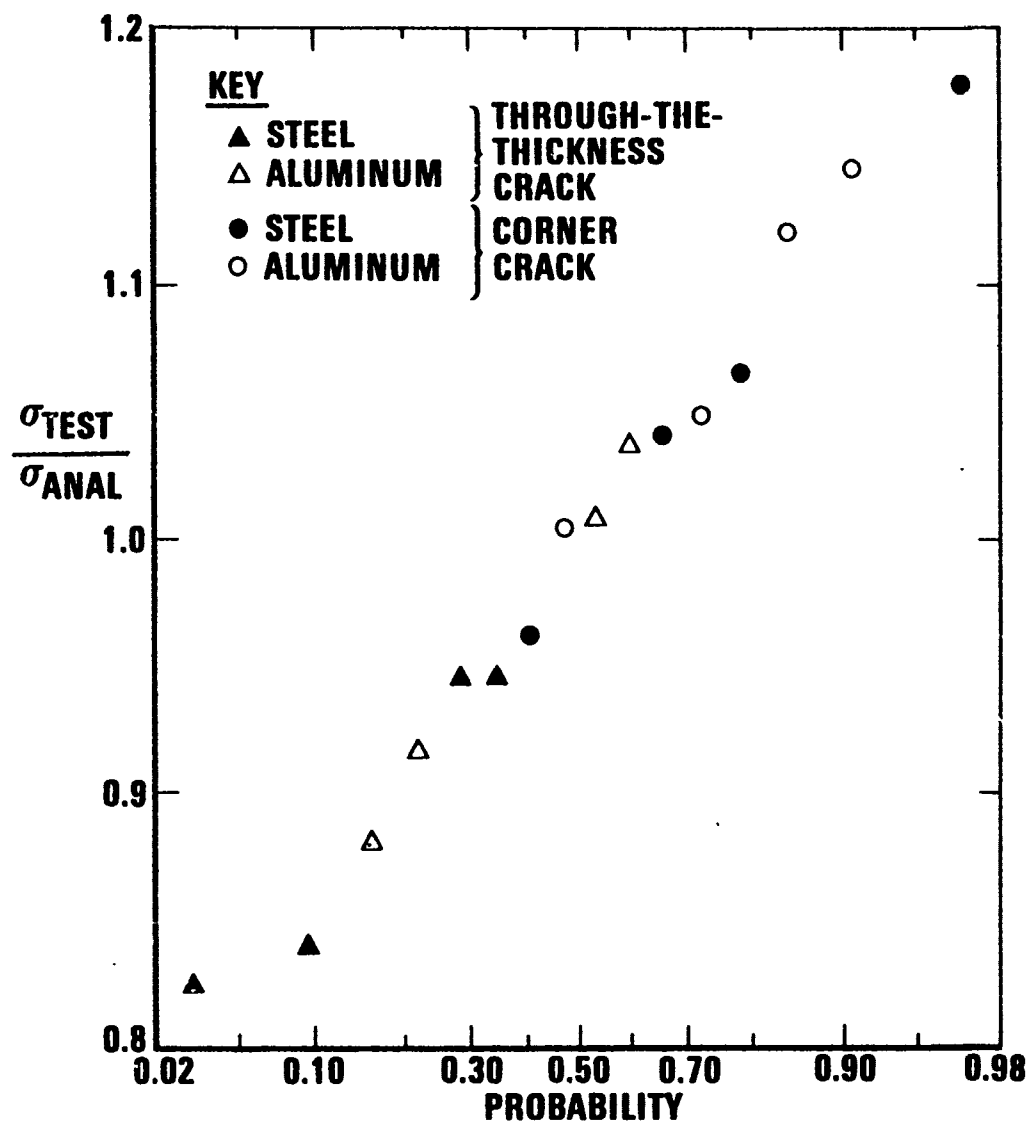


Figure 4-2. Accuracy of Residual Strength Predictions for Group I Tests

Final failure of lugs following fatigue crack growth testing also tended to be by a net-section yielding phenomenon rather than by exceedance of a critical stress intensity factor value for most of the specimens. The exceptions were the specimens loaded so that the peak stress at the lug hole was above the yield strength of the material.

For through-the-thickness cracks, the 2-D finite element method and Green's function method are found to be reliable and versatile. The compounding method also gave excellent performance, especially in the context of the simplicity of the method. The compounding method predicted conservative lives for $R_0/R_1 = 1.5$ and unconservative lives for $R_0/R_1 = 2.25$ and 3.0 when compared with the Green's function method. Efforts to improve the compounding method were unsuccessful. However, one can use the compounding method with reasonable confidence to predict life, at least as a first approximation when no other solutions are available. This program recommends, however, the use of the Green's function method for more accurate predictions of crack growth behavior and life. A typical result of a through-the-thickness crack growth behavior in an aluminum lug subjected to constant-amplitude loading with analytical predictions by the compounding and the Green's function methods is given in Figure 4-3.

For corner crack problems, the two-parameter corner crack correction factors modifying the through-the-thickness crack solution are found to make excellent predictions for the crack growth behavior and life. The predictions of crack aspect ratio, a/c , can be considered only satisfactory. The actual a/c ratios were slightly higher than predicted. The one-parameter corner crack approach also yielded reasonable crack growth and life predictions, but is also only approximate since the experimental aspect ratios were not constant as assumed in this approach. A typical corner crack result is given in Figure 4-4.

The experimental data scatter in the aluminum lugs at both stress levels, 6 and 15 ksi, is very minimal for R_0/R_1 ratios of 2.25 and 3.0, but is larger for the R_0/R_1 ratio of 1.5. The authors believe that this may be due to the fact that these smaller lugs have high stress concentrations, which may make them very sensitive to parametric variations, for example the loading pin-lug clearance.

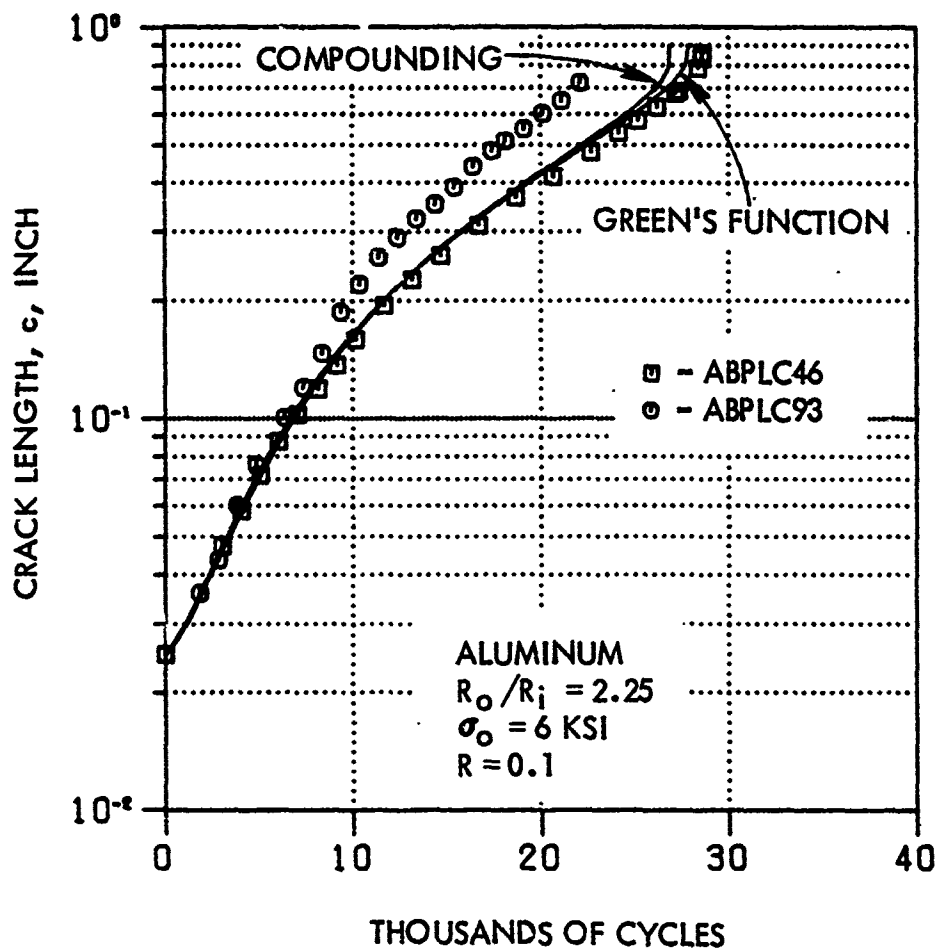


Figure 4-3. Through-the-Thickness Crack Growth Data and Prediction, Aluminum Lug, $R_o/R_i = 2.25$, $\sigma_o = 6$ ksi, $R = 0.1$

4-2

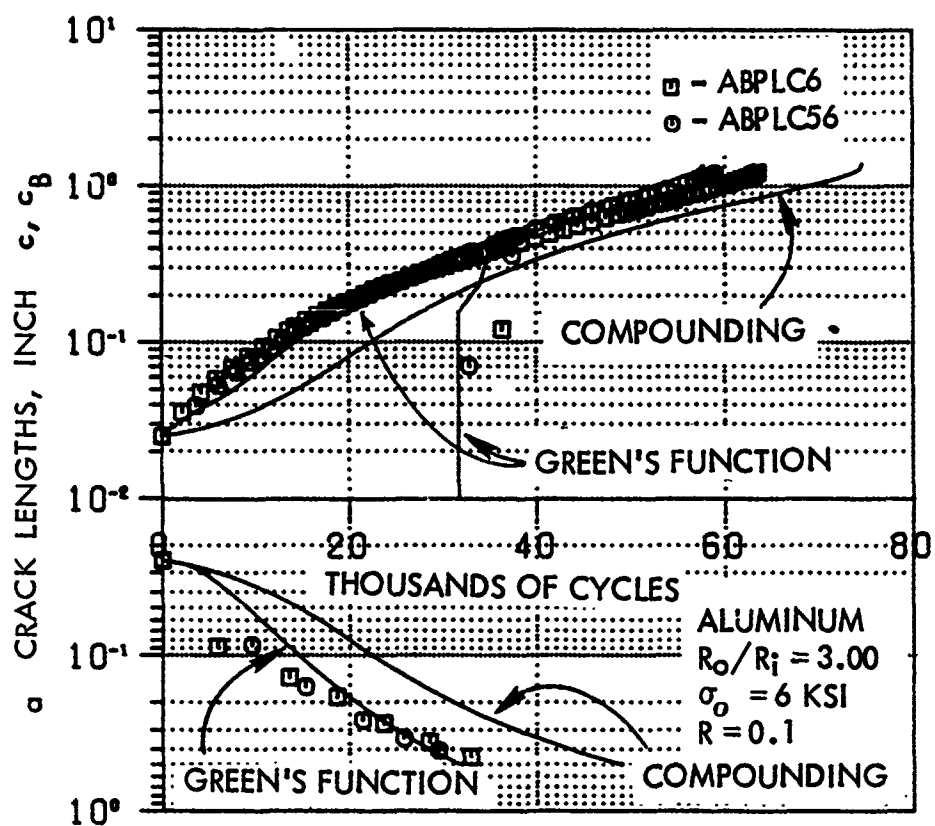


Figure 4-4. Corner Crack Growth Data and Prediction, Aluminum Lug, $R_o/R_i = 3.0$, $\sigma_o = 6 \text{ KSI}$, $R = 0.1$

The authors also believe that the pin-to-lug rigidity ratio, $E_{\text{pin}}/E_{\text{lug}}$, and large deformation of the lug due to pin loading may have influenced the crack growth behavior and life. However, such effects were predominant only in small lugs with $R_0/R_1 = 1.5$ and diminished as the R_0/R_1 ratio was increased.

Failure of corner crack specimens was predicted prior to transition for $R_0/R_1 = 1.5$, but transitional and subsequent through-the-thickness crack growth behaviors were predicted for $R_0/R_1 = 2.25$ and 3.0 . In almost all cases this agreed with the experimental results. Figure 4-4 also shows a sample correlation of experimental and analytical predictions of transitional and through-the-thickness growth of initial corner cracks.

In the cases of lug specimens subjected to load levels that induced peak local stresses above the yield strength of the material, there were many difficulties in conducting these tests including premature failure and the presence of a large number of natural cracks. The analysis procedure developed using the Green's function and the elasto-plastic stress distribution was also found to be inaccurate as shown in Figure 4-5. Also, the analysis predicted increasing life as R_0/R_1 increases, whereas the experimental data for initial through-the-thickness cracks (but not for initial corner cracks) show the opposite trend of increasing life as R_0/R_1 decreases. The correlation could have been improved further by the use of cyclic stress-strain data instead of the monotonic stress-strain data used in the analysis. Even such an improvement may not have been sufficient to explain the above phenomenon and one may have to resort to the use of special plastic crack-tip elements embedding the HRR (Hutchinson-Rice-Rosengren) type singularity.

In all the spectrum loading cases, the Hsu and the Generalized Willenborg retardation models predicted almost identical crack growth behavior and lives. These models predicted solutions which were in excellent agreement with experimental data for most of the cases as depicted in Figure 4-6. The solutions were unconservative only for steel specimens subjected to fighter spectrum loading, and no reasonable explanation could be found for this discrepancy. The Willenborg model results were unconservative by a factor of about 2 to 5 when compared with Hsu or Generalized Willenborg model. The no-retardation model predicted lives which were about half of the lives predicted by the Hsu or the Generalized Willenborg model.

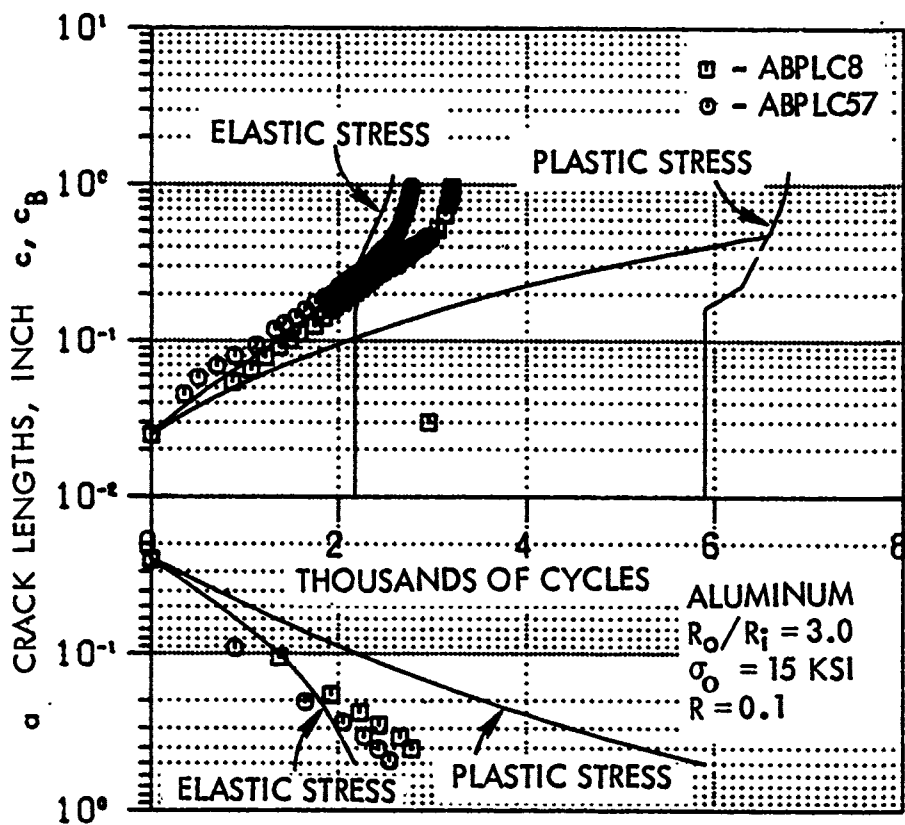


Figure 4-5. Corner Crack Growth Data and Prediction, Aluminum Lug, $R_o/R_i = 3.0$, $\sigma_o = 15$ KSI, $R = 0.1$

- [A] HSU
- [B] GENERALIZED WILLENBORG
- [C] WILLENBORG
- [D] NO RETARDATION

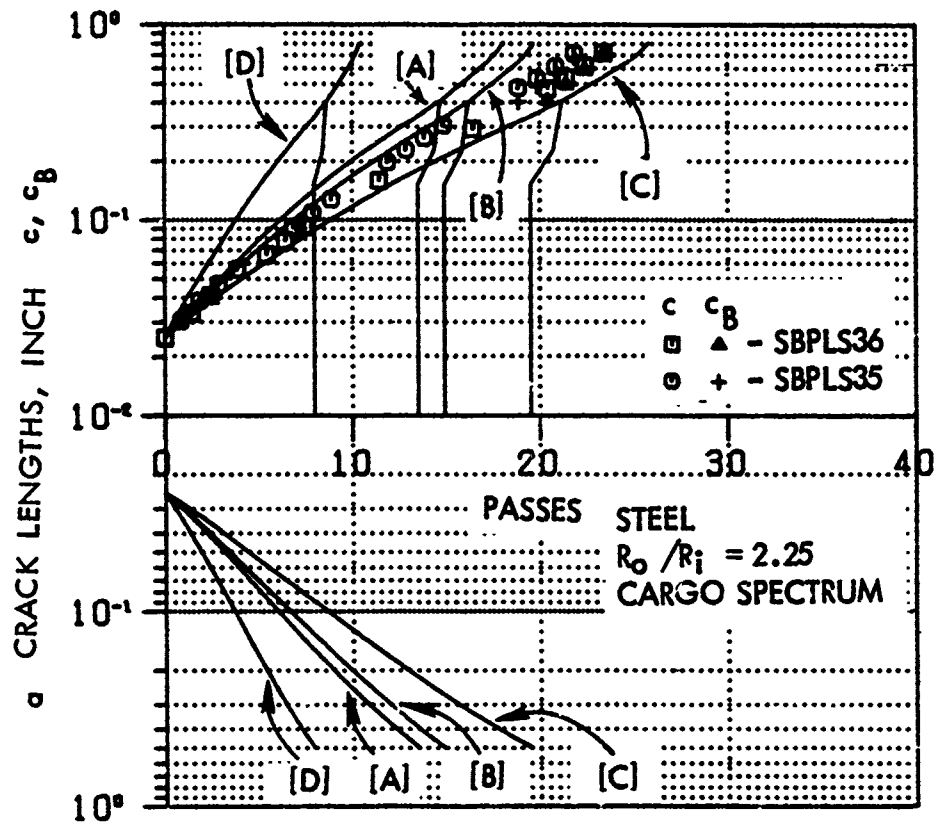


Figure 4-6. Corner Crack Growth Data and Prediction, Steel Lug, $R_o/R_i=2.25$, Cargo Spectrum Loading

The blunting installation procedure introduced some blunting of the crack tip due to the high interference levels. This in turn sometimes retarded the initial crack growth and resulted in conservative life predictions.

Extensive experimentation was made to select block and flight-by-flight spectra which would introduce markings on the fracture surface so that the corner crack aspect ratio could be monitored. Such efforts were unsuccessful due to the constraints imposed by the present program. However, maximum information was extracted from these tests by monitoring the back surface crack lengths after the crack had broken through the thickness.

Figure 4-7 shows the accuracy of crack growth life predictions for all the 160 Group I crack growth specimens. Here each data point is the geometric mean of duplicate test results. This figure indicates that approximately 98 percent of crack growth life predictions for straight lugs would be within a factor of 3.0 of the test results. Of the 160 test results, the life ratios for 126 results fall within the band of 0.5 to 2.0. Giving allowance for some of the analytical and/or experimental difficulties cited above, a very satisfactory performance of all the analytical methods developed in this program is indicated by this correlation.

3. RESULTS AND CONCLUSIONS FROM GROUP II TESTS

Crack growth life of a lug is longer if the pin clearance is smaller, based on tests of lugs with nominal diametrical pin clearances of 0.0005 inch, 0.0015 inch, and 0.0030 inch. Results for straight lugs are shown in Figure 4-8. Note that lubricant applied to the pin before testing failed to have the expected beneficial effect. Apparently, judging from fretting evidence, the lubricant did not significantly reduce the frictional shear stresses at the pin-lug interface.

For the same magnitude of axial load and the same R_0/R_1 ratio, the crack growth life of a tapered lug is longer than that of a straight lug, which is consistent with analytical prediction. The life of a dogbone-shaped lug is somewhat shorter than that of a straight lug, but the

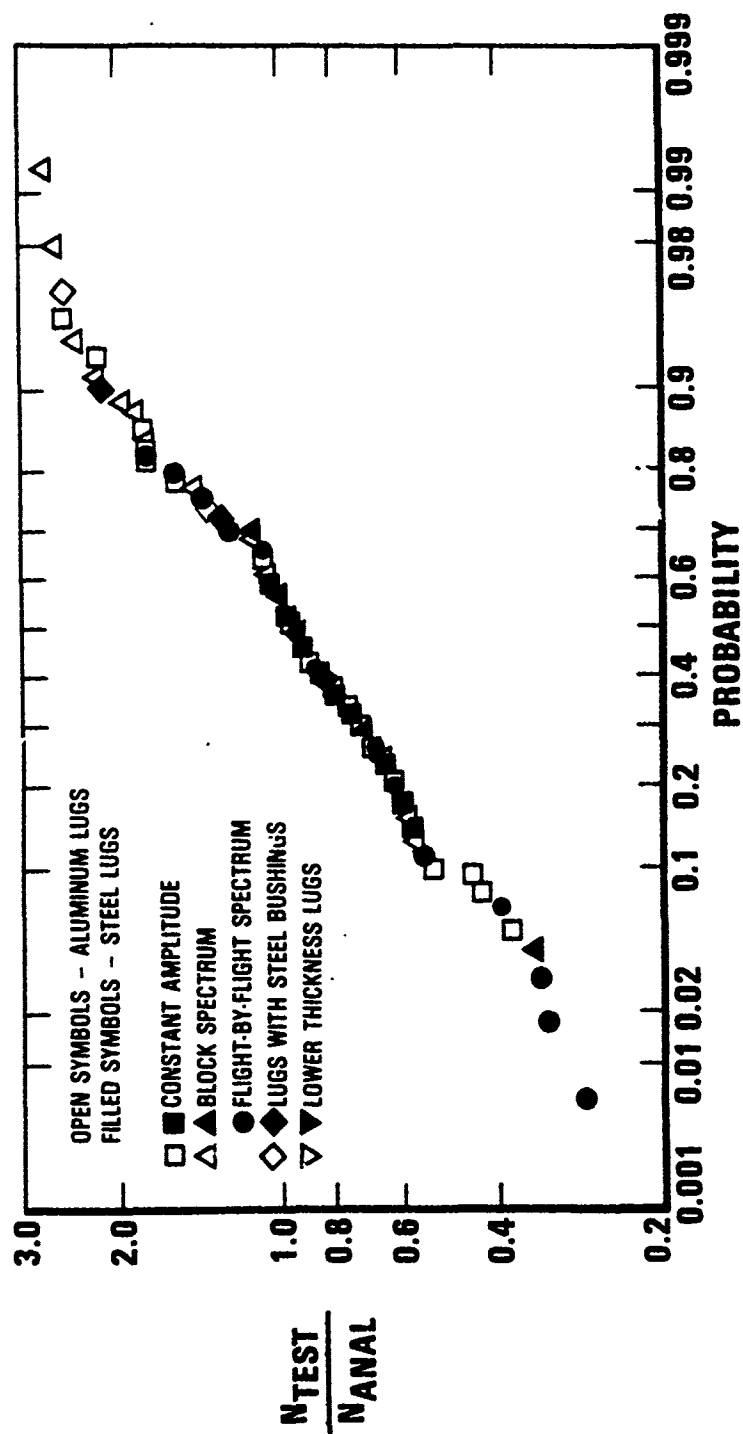


Figure 4-7. Accuracy of Predictions of Total Crack Growth Life for Group I Tests

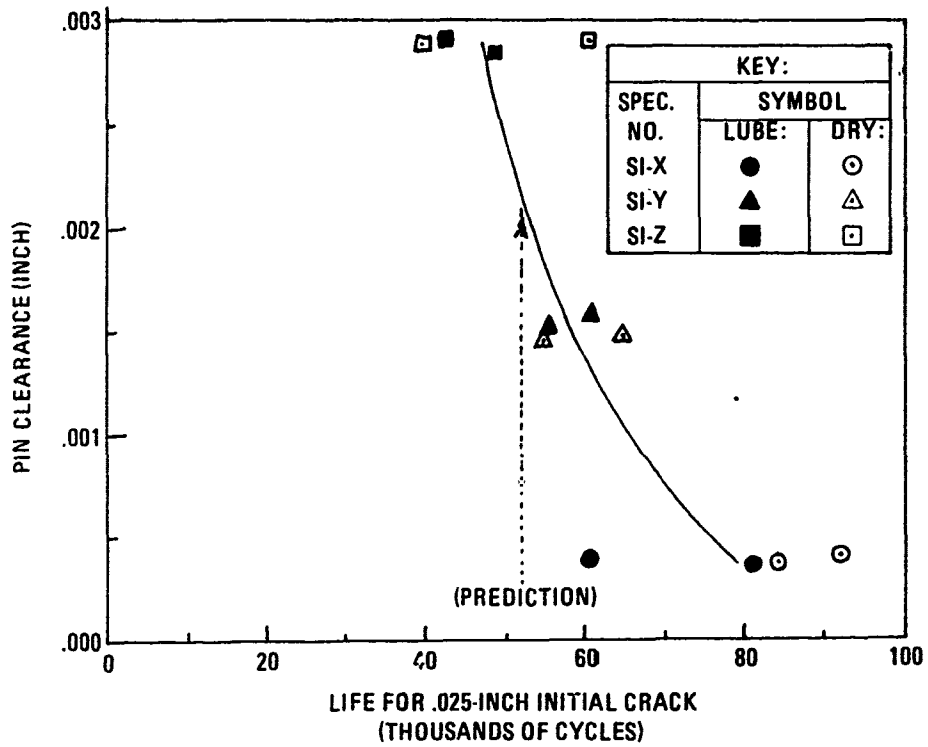


Figure 4-8. Results of Pin-Clearance Study, Axially-Loaded Straight Lugs

9 straight lug analysis can be used as an approximation. These test life comparisons are shown in Figure 4-9.

A steel shrink-fit bushing in an aluminum lug, with typical production interference of $\Delta r/r = 0.0020$, will tend to separate from the lug when loaded. If this separation is not accounted for in the analysis, growth life can be overestimated by a large factor (4.4 to 22 in these tests). Separation can be conservatively represented by modeling the pin and bushing together as a larger (frictionless) pin. Figure 4-10 shows a typical example of the data and the two predictions, with and without considering separation at the lug-bushing interface.

Stress intensity factors obtained from crack-tip finite element analysis of off-axis-loaded tapered lugs were available for $c/(R_0 - R_1) \leq 0.95$. Within this range, crack growth predictions tended to be mildly conservative. Crack growth in off-axis loaded tapered lugs was complicated by the following phenomena, as observed in Figure 4-11:

- o The cracks grew to lengths far beyond the range covered by FEM analysis, necessitating major extrapolation of the K vs. c relationship.
- o Crack growth was non-radial and non-coplanar, especially in steel (but in aluminum also).
- o There was a tendency for the crack to branch in an alternative direction. Usually the secondary crack would cease propagating, prolonging the growth life of the primary crack. However, in steel specimen No. T1-S-4 the growth of the secondary crack eventually caused specimen failure.

Despite these complexities the life predictions for these specimens were normally within a factor of 2 of the test results and tended to be conservative. Predictions for the steel lugs were especially accurate.

The shrink-fit steel bushings in the off-axis loaded steel tapered lugs had a very small effect on crack growth. Although bushing-lug separation may have occurred, it did not strongly effect either predicted or test life like it did in aluminum lugs with steel bushings (wherein the bushing-to-lug modulus ratio was 3:1).

In thick, axially loaded straight lugs the crack tended to turn out of plane as seen in Figure 4-12 shortly after the corner crack had become an

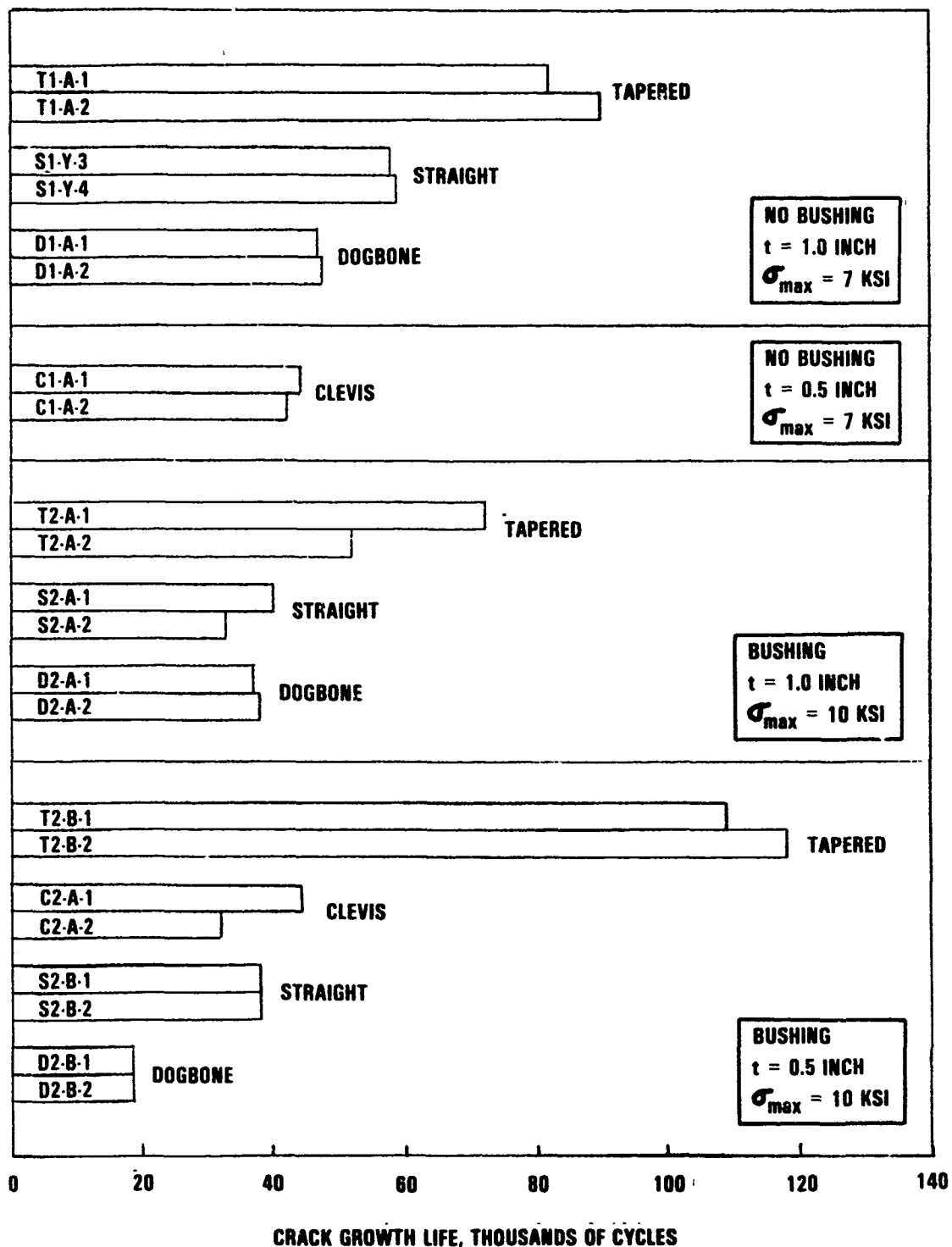


Figure 4-9. Effect of Lug Geometry on Crack Growth Life

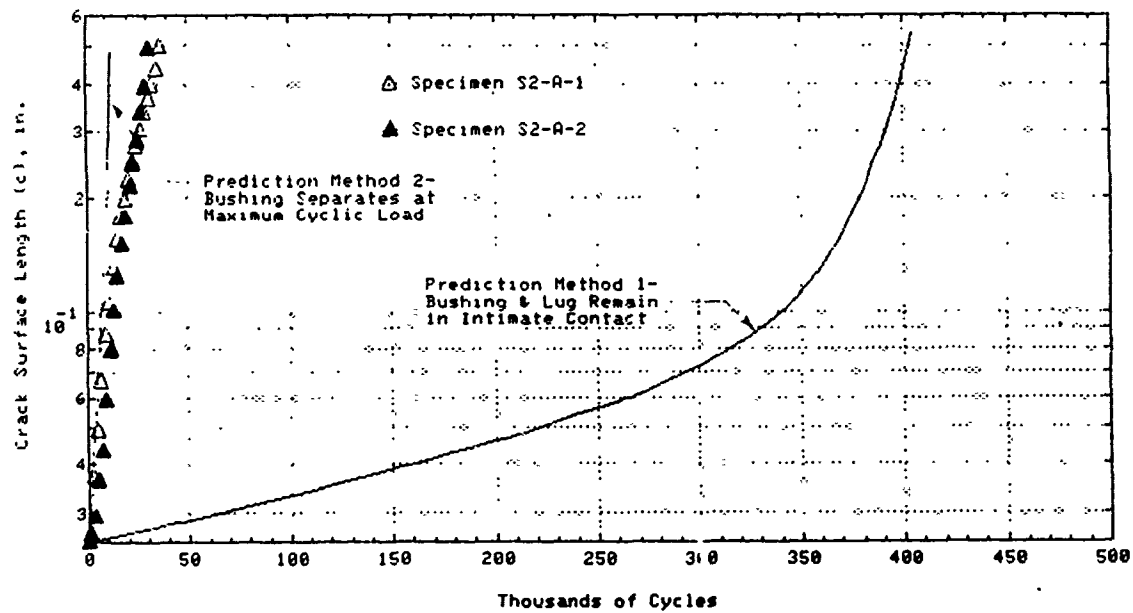


Figure 4-10. Comparison of Two Analysis Methods for Lugs With Shrink-Fit Bushings

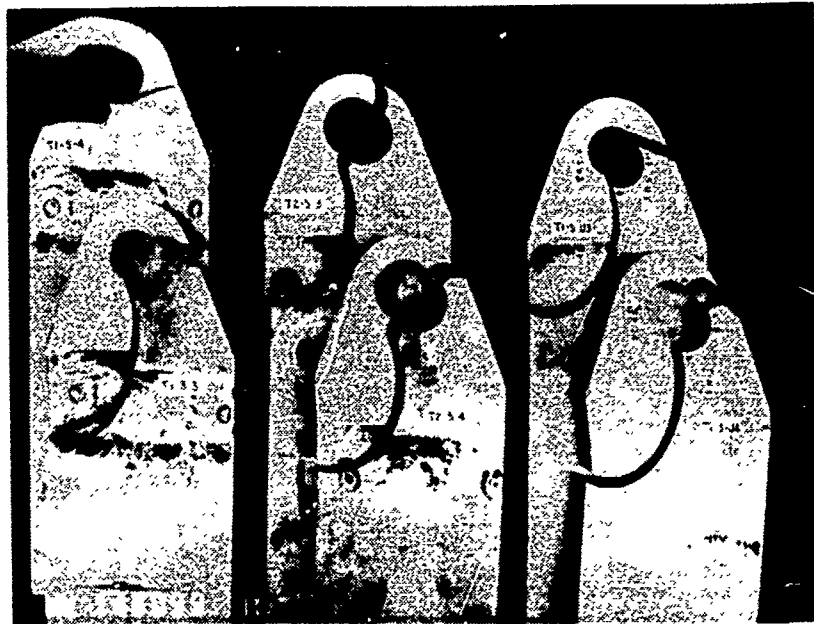


Figure 4-11. Crack Profiles for Steel Tapered Lugs Loaded in the -90 Degree Direction

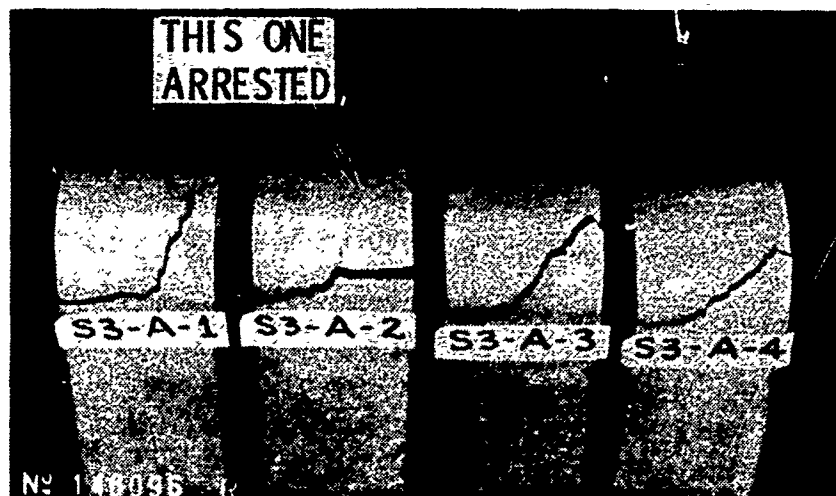


Figure 4-12. Crack Curving and Secondary Cracks in Specimens S3-A-1 through -4

across-the-ligament crack. Subsequently the turned crack tended to slow down and stop, necessitating the initiation of a second crack to bring about lug failure. This added test life contributed to the conservatism of the analysis of these specimens.

Even while a corner crack, the crack growth predictions for the thick straight lug specimens were somewhat inaccurate. As Figure 4-13 shows the magnitudes of the errors in prediction were similar for spectrum loading and constant amplitude loading, but differed for different lug sizes.

The redundant wing-pylon lug analysis required special finite element modeling to account for the lug shape, effects of fasteners and structural supports, and effects of a shrink-fit bushing including separation at the lug-bushing interface. The Green's function for an axially loaded straight lug had to be used for this complex geometry without modification. Spectrum loading was applied, requiring use of the Hsu retardation model. No account was taken for redundancy of the lug or load transfer between the cracked and uncracked member.

The fracture surface of one wing-pylon attach lug specimen is shown in Figure 4-14. This figure describes an annotated record of the failure sequence, showing the initial crack location (I.C.), and sequence of events (failure or crack initiation) with encircled numbers along with corresponding flight numbers or locations of crack fronts. Figure 4-15 is a plot of crack length versus flights for the two wing-pylon specimens tested. The ordinate shows the position of the lug hole and the locations of the cracks on both sides of the hole in both pieces of both specimens. Also included in this figure is the growth prediction for the initial crack until failure of the first ligament. Despite the complexities discussed above, this prediction was accurate within a factor of 2.0. Note, however, that failure of the first ligament did not cause immediate failure of the lug. On the contrary, the total test lives were approximately 2.5 times the time to first-ligament failure. These tests show dramatically the damage-tolerance advantages that can be obtained in a redundant design if the initial crack occurs in only one member. The specific advantages apparent in Figure 4-15 are:

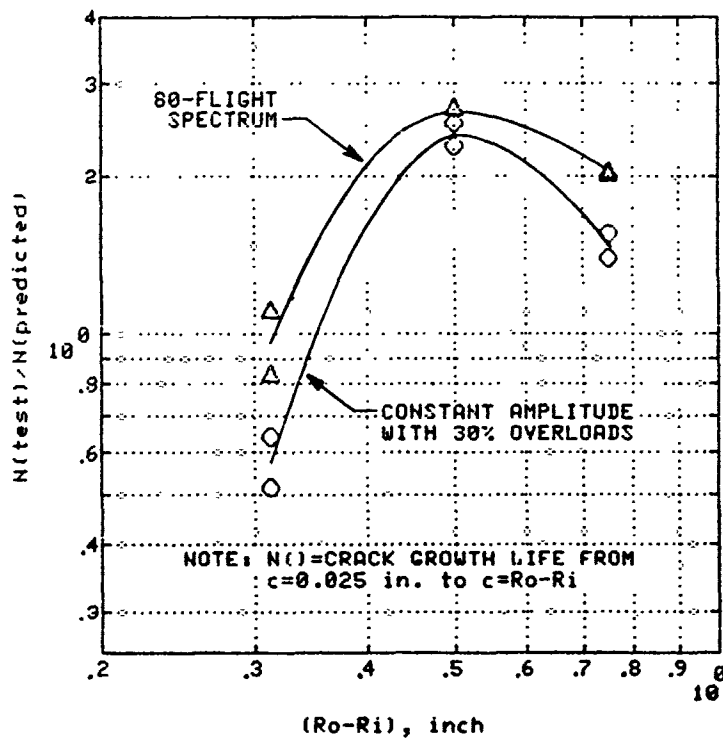


Figure 4-13 Correlation of Test and Predicted Crack Growth Lives Before Transition for a Corner Crack in Thick Straight Lugs

4.13

49

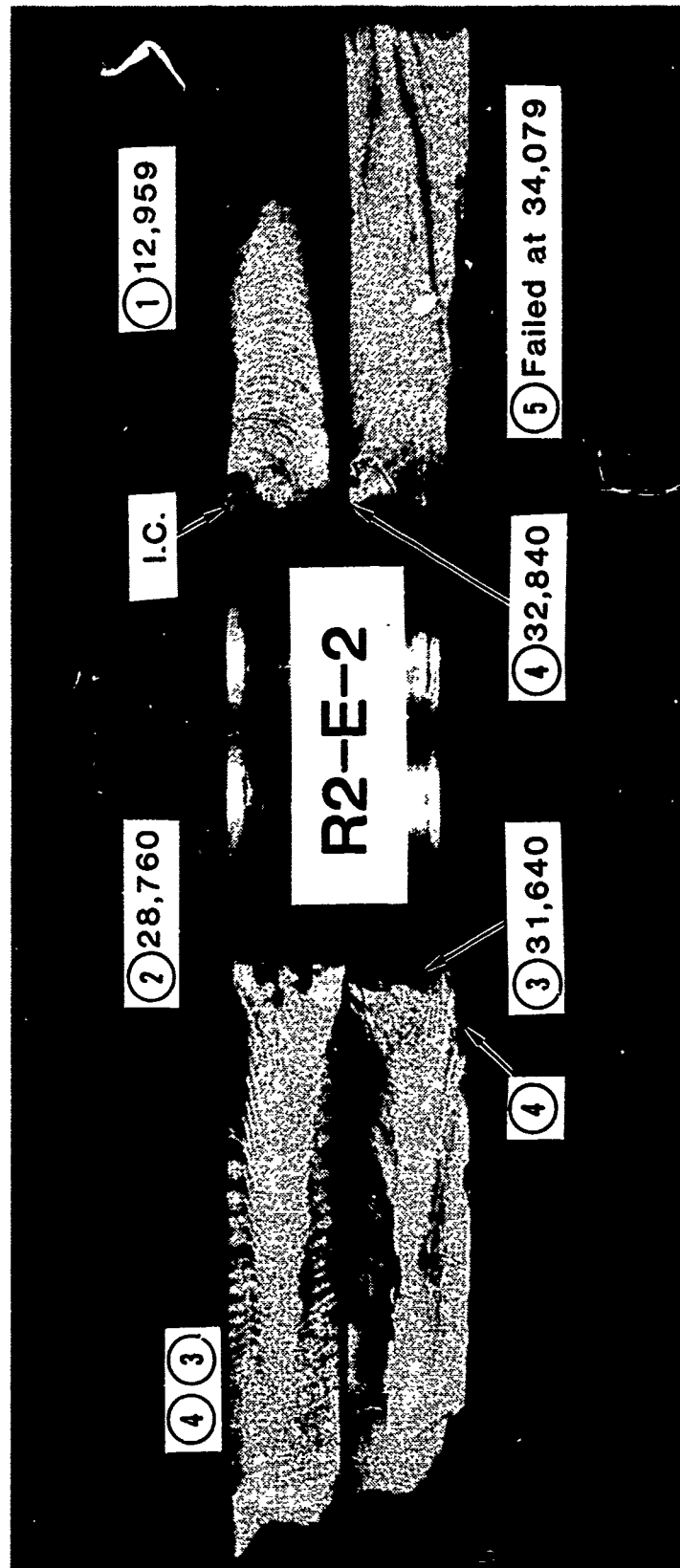


Figure 4-14. Fracture Surface of Simulated Wing-Pylon Lug Specimen R2-E-2

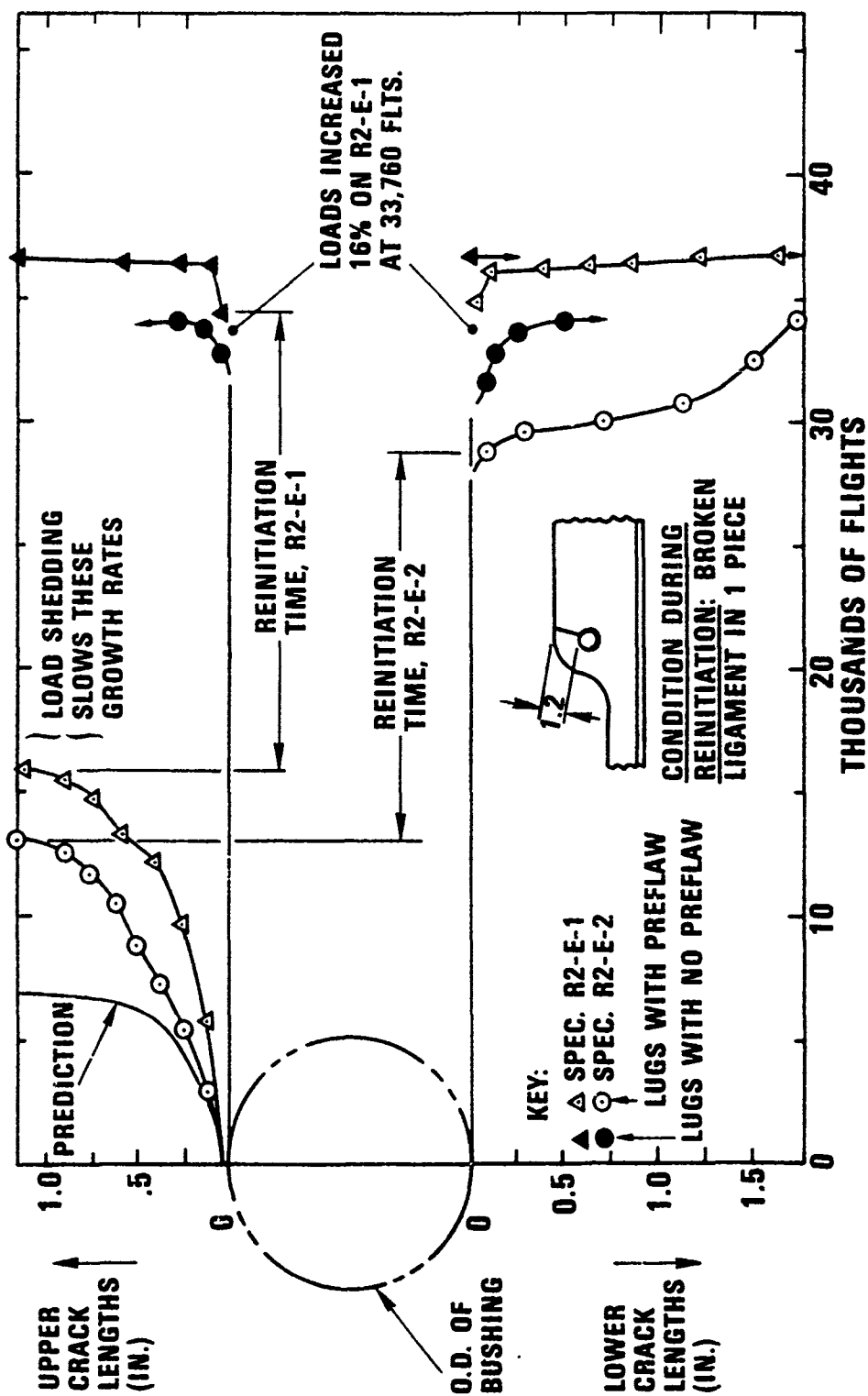


Figure 4-15. Crack Growth in Simulated Wing-Pylon Specimens R2-E-1 and R2-E-2

- o The remaining life after failure of the initial ligament exceeded the crack growth life prior to ligament failure, because of a very long crack reinitiation period.
- o The damage condition throughout this reinitiation period was a broken 1.2 inch ligament, which would be highly inspectable.
- o The crack growth rate prior to ligament failure was reduced due to load shedding to the neighboring member.

It is apparent that these advantages would disappear in the event of a compound misfortune in which both members in the redundant lug were pre-flawed equally.

Figure 4-16 shows the ratio of test life to predicted life for all Group II specimens. The analytical predictions range from accurate to conservative. Note that nine of the 10 most conservative predictions are for aluminum lugs with steel bushings with standard manufacturing interferences. These analyses were done allowing for separation between the lug and bushing, during loading, and the consistent conservatism results from the modeling of the pin and bushing together as a larger (frictionless) pin. When lug-bushing separation was not allowed in the analysis, the predictions were unconservative by factors of 4.4 to 22.

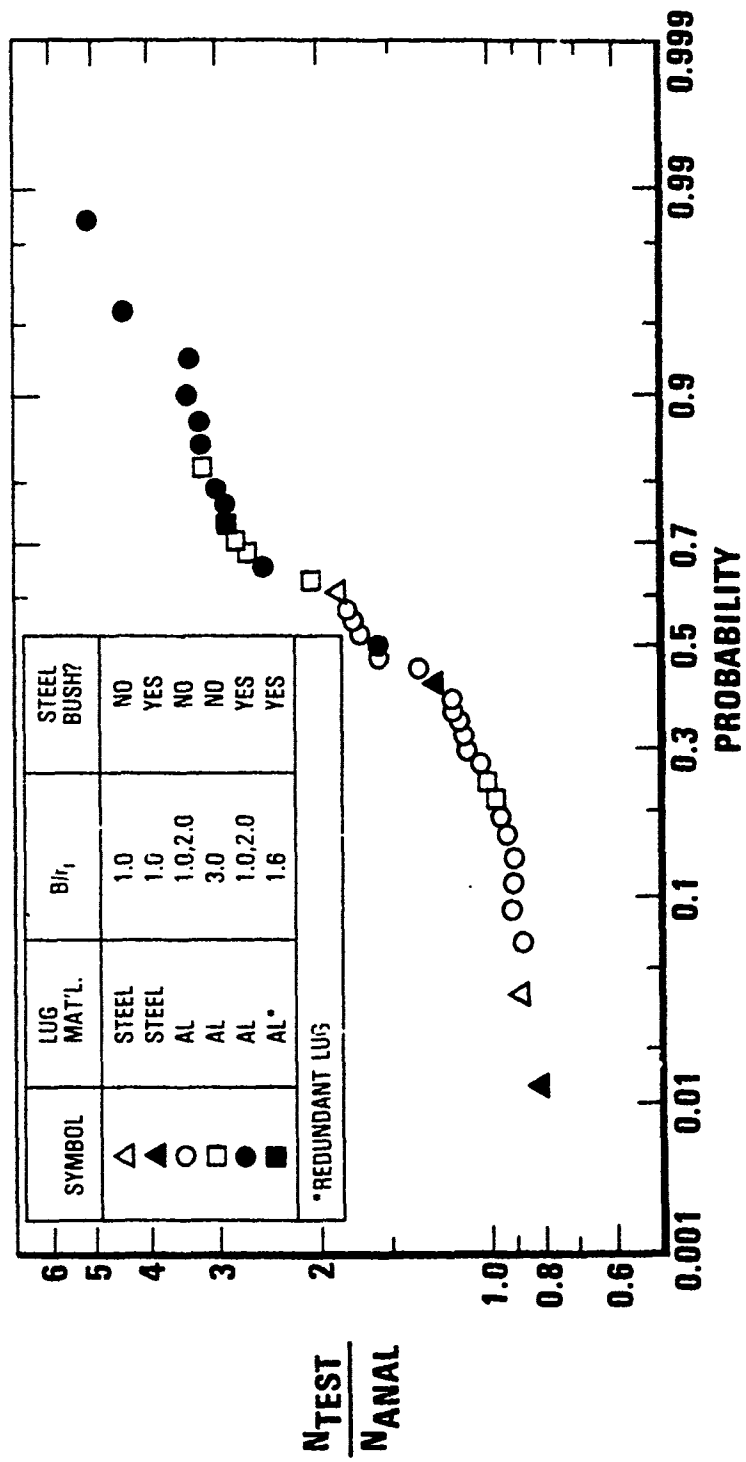


Figure 4-16. Accuracy of Predictions of Total Crack Growth Life for Group II Tests

SECTION V

CRITERIA ASSESSMENT

Initial flaw requirements for damage tolerance design analysis of aircraft attachment lugs are recommended in this section. These recommended requirements have been developed specifically for problems of fatigue cracking and based on fatigue crack growth testing and analysis. Therefore, materials and structure that are significantly more susceptible to sustained load stress corrosion cracking than they are to fatigue cracking are excluded from consideration in these recommendations. For example, landing gear lugs made from ultra-high strength (260-280 ksi) steel are excluded.

Reference [6] provides the precedents for damage tolerance design requirements for metallic aircraft structure. At a fastener hole, a 0.050-inch radius quarter-circular corner crack must be assumed to exist at the time of manufacture at the most critical location. This size was originally selected by the collective engineering judgment of industry and Air Force experts, and then [8] verified to be consistent with NDI limits for 90 percent reliable detection with 95 percent confidence. Besides protecting against undetectable crack-like defects, the 0.050-inch crack was considered sufficiently severe to protect against other types of possible undetected defects such as material inclusions and tool marks. Since hole drilling was considered a major source of preflaws at fastener holes, adjacent members that are both drilled together in a single operation are assumed to both contain 0.050-inch radius corner cracks at the same location. Additional 0.005-inch radius continuing damage corner flaws are required at neighboring fastener holes as a conservative way to represent virgin fatigue quality.

1. INITIAL FLAW TYPE AND SIZE FOR LUGS

A corner crack is a common initial crack type in attachment lugs. In fact, Task I showed that, for lugs which failed by fatigue crack growth, the corner crack was the most common crack type.

Lugs tend to be more highly loaded than fastener holes. This is confirmed by the small critical crack sizes found in the Task I cracking data survey (Figure 2-3). Since it is desired to avoid undue weight penalties when damage tolerance design criteria for lugs are introduced, there is a desire to justify the use of smaller assumed initial crack sizes for lugs than the 0.050-inch crack.

During the Task II evaluation of NDI methods, it was noted that the automatic eddy current method for aluminum and magnetic rubber method for steel are both capable with good reliability of finding cracks of approximately 0.025 inch length, measured radially. Furthermore the potential exists to enhance the reliability of NDI for these sizes by any of several approaches, including improved training of inspectors and the use of multiple independent inspections. It can also be argued that inspection of a lug might, by nature, be more intensive and hence more reliable than inspection of fastener holes, in view of the large number of fastener holes in a typical aircraft joint that must be inspected. This more intensive inspection should result in equivalent reliability for a lug for a smaller crack size, compared to fastener holes.

Regarding crack shape, data from Task V testing and from the Task I survey indicate that corner cracks in lugs tend to be deeper than long by a factor of 1.3 or more. However, there is a precedent [6] for using a simple quarter-circular shape. A quarter-circular shape is less ambiguous to apply at other than a 90-degree external corner, such as the beveled corner commonly used in lugs. Consequently a standard assumption of 0.030-inch quarter-circular initial corner crack is recommended as the initial flaw requirement for single attachment lugs.

It is emphasized that no quantitative statistical NDI data on lugs were found in the Task II survey. A thorough verification program paralleling that of Reference [8] would be needed to substantiate that this flaw size can be detected in lugs with 90 percent probability and 95 percent confidence.

However, inspectability alone is inadequate to justify initial flaw sizes for damage tolerance requirements for attachment lugs. In the cracking data survey summarized in Section II, only six of the 55 service

fatigue failures of lugs could be traced to initial defects. Improved initial inspection could have done nothing to prevent the other 49 failures. Thus, considerations other than inspectability are necessary if the criteria are to have the desired effect of reducing the number of fatigue failures. These other considerations include manufacturing quality, which prevents the occurrence of rogue defects or limits their size.

In addition to the possibility of more careful inspections, manufacturing quality is more closely controlled for a lug than for large-scale mechanically fastened structure. The fixed, hard tooling used in reaming or boring, with controlled feed and speed and the use of coolant, must be used in order to achieve the close-tolerance holes required for lugs. The machines are designed for precision work, are carefully maintained and are operated by experienced craftsmen.

In recommending the 0.030-inch initial crack, the authors assume that damage tolerance critical lugs will not only be carefully inspected, but also carefully manufactured. Like the 0.050-inch crack at a fastener hole, it is assumed that the 0.030-inch crack in a lug is severe enough to protect against other types of undetected defects such as inclusions and tool marks.

2. FLAW MULTIPLICITY FOR REDUNDANT LUGS

An intent of damage tolerance requirements is to protect against the worst reasonably possible case. Fatigue tests of lugs commonly show multiple crack origins [1]. Therefore flaw multiplicity must be considered. The precedent for mechanically fastened redundant structure other than lugs [6] is to assume an equal corner crack in each member where the fastener hole is produced simultaneously in both members by a common drilling operation.

Data from tests in this program (Figure 4-15) and in the literature [9] have dramatically demonstrated the potential benefits of redundant lug design, provided that only one member contains a preflaw. First, the crack growth rate is slowed due to load shedding from the cracked member to the uncracked member. Secondly, after the first ligament breaks there is an initiation period that precedes further cracking; in the tests in this

program (Figure 4-15) the duration of the initiation period exceeded the prior crack growth period, which more than doubled the crack growth life. Thirdly, throughout that long initiation period the existing damage in the lug (a broken ligament) is highly inspectable.

However, if the precedent in [6] were followed in requirements for lugs, equal 0.030-inch-radius corner cracks would be assumed in each member of a redundant lug, because alignment of the holes requires that the finishing operation on the lug hole be done to both pieces simultaneously after assembly. Then, if both pieces were assumed equally cracked, the benefits of redundancy would be lost and the two-piece design would actually become worse (by calculation) than the comparable one-piece design.

Although obviously conservative, this may not be the best initial flaw assumption for redundant lugs. The rogue defect by definition has an extremely remote probability of occurrence. Therefore the probability of two simultaneous rogue defects at the two adjacent worst locations seems too unlikely to use as the focal issue that decides the acceptability or unacceptability of the lug design.

The multiple origins that were noted in [1] resulted, not from two coincidental crack-like rogue defects, but from fatigue initiation of virgin (unflawed) lugs. The 0.005-inch radius crack is used in [6] to represent virgin fatigue origins, but for that purpose can be quite conservative. Results of past tests [10], demonstrating this conservatism, are shown in Figure 5-1. Five sets of fastener hole specimens were fatigue tested. Within each set were three groups of specimens. A 0.005-inch corner crack at a hole was fatigue-induced into each specimen of the first group. A 0.020-inch-deep scratch was introduced at the corresponding location of the specimens in the second group, using diamond paste abrasive and a gentle sawing action to minimize the favorable residual stresses. Therefore, these flaws were conservative representations of actual machine marks, which would be not as deep and have high residual stresses. Specimens in the third group were not preflawed. Under identical fatigue loading, the specimens with initial corner cracks and those with razor blade flaws had equal fatigue lives, and significantly shorter lives than the unflawed specimens. Thus, these tests showed that not only were the .005-inch cracks very conservative for representing unflawed holes, but also for

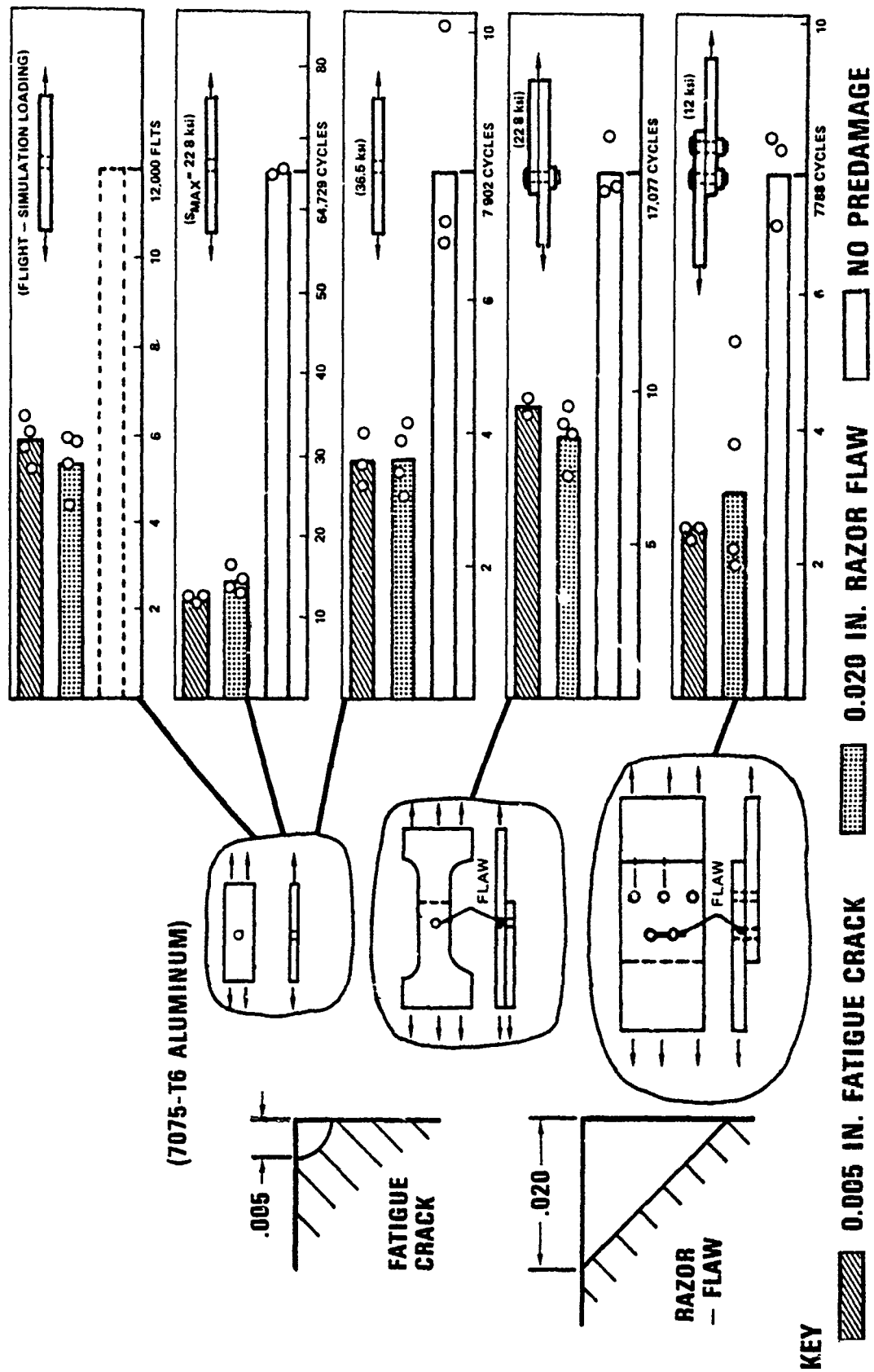


Figure 5-1. The Equivalence of a Deep, Sharp Scratch and a 0.005-Inch Corner Crack

representing flaws such as scratches or machine marks, which are not crack-like.

The authors suggest that the key to the dilemma of redundancy versus crack multiplicity is to recognize that there are two different types of initial defects - the crack-like rogue defect, and those flaws which occasionally occur in multiples but are not crack-like - and to consider them separately. Therefore, a candidate requirement is recommended for redundant lugs by which the more severe of the following two assumptions is made:

- (a) One 0.030-inch radius quarter-circular corner crack is assumed in the worst location of one member, representing a rogue defect. Typical initial fatigue quality is assumed in all other members.
- (b) All adjacent members including the primary member are assumed to contain equal 0.005-inch quarter-circular initial corner crack.

In general, relevant fatigue data are needed to quantitatively define "typical initial fatigue quality" in Assumption (a). In the absence of such data, a 0.005-inch initial quarter-circular corner crack is assumed in each secondary member, in which case Assumption (a) (being the more severe) will pre-empt Assumption (b).

The current analysis method for predicting secondary cracking in conjunction with Assumption (a) is the Equivalent Initial Quality Method [11]. By this method fatigue life data are used with the help of fractographic data to back-calculate an equivalent initial flaw size which represents typical initial fatigue quality. This initial flaw size is then assumed in all secondary members of a multi-load-path lug per Assumption (a). The growth of this flaw is predicted using a growth rate relationship consistent with the relationship used with the original fatigue data to back-calculate that flaw size in the first place. Of course, alternative analysis methods such as the method described in Reference [12] should not be ruled out if they can be shown to be sound.

The 0.005-inch cracks in Assumption (b) are intended to conservatively represent any defects that, if present, are likely to occur equally in both members. Two examples are unexpected early fatigue or fretting cracks, or scratches which occur while reaming or boring the lug hole or installing

the bushing. The 0.005-inch size is based upon engineering judgement which assumes care in manufacturing of attachment lugs, and upon the data shown in Figure 5-1.

This dual criterion would give appropriate credit for the redundancy, but also would protect against all reasonably possible sources of single or multiple defects. The authors recognize that this proposed criterion differs from the approach of [6], which has existed for over 10 years. However, during those 10 years there has been a sustaining concern that the use of redundant structure, which was long regarded as the most damage tolerant structural concept, is discouraged by the criteria. These recommendations, if accepted for lugs, may provide a proving ground for later improvements of MIL-A-83444 for all aircraft structure.

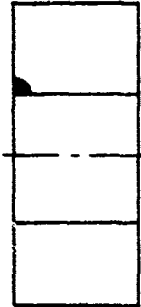
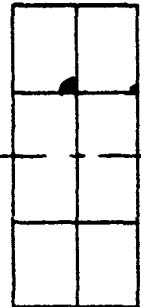
3. SUMMARY OF INITIAL FLAW RECOMMENDATIONS

Table 5-1 summarizes the recommended initial flaw sizes for damage tolerance analysis of attachment lugs. For single lugs the recommended initial flaw size is a quarter-circular corner crack with a radius (r) of 0.030-inch. For multi-piece lugs, the recommended initial flaw conditions are either (1) a quarter-circular corner crack of $r = 0.030$ -inch in one piece and the other pieces have typical initial fatigue quality, or (2) quarter-circular corner cracks of $r = 0.005$ -inch in all pieces; whichever is more severe.

The 0.030-inch crack size is intended to be consistent with inspection capabilities for crack-like defects in lugs corresponding to a 90 percent probability of detection and a 95 percent confidence limit, and is intended to be severe enough to protect against other types of unrepaired defects such as inclusions and tool marks. The 0.005-inch cracks are intended to be as severe as any initial flaw that has a reasonable possibility of occurring in multiples in redundant lugs, due to causes such as fatigue, fretting, scratches, etc.

Thus, these candidate recommendations are made assuming extreme care in both manufacturing and inspection of potentially damage tolerance critical attachment lugs.

TABLE 5-1. RECOMMENDED DAMAGE TOLERANCE INITIAL FLAW SIZE REQUIREMENTS FOR LUGS

LUG TYPE	Single Lug	Redundant Lug	
			
NUMBER OF REQUIREMENTS	One Requirement	Two Requirements*	
		Requirement 1:	Requirement 2:
NUMBER OF QUARTER-CIRCULAR CORNER CRACKS:	One	Two	Two
RADIUS OF EACH INITIAL CRACK	0.030 Inch	Primary: 0.030 Inch Secondary: 0.005 In. or Smaller Size Established by Data	0.005 Inch
DEFECT TYPES REPRESENTED (and DEFECT SOURCES)	Undetected Crack-Like Rogue Defect (Material or Heat-Treatment Defects)	Primary: Undetected Crack-Like Rogue Defect (Material or Heat-Treatment Defect) Secondary: Typical Initial Fatigue Quality	Initial Flaws Which Tend to Occur in Equal Pairs — Not Crack-Like (Fatigue; Fretting; Scratches From Hole Preparation or Bushing Installation)

*Both requirements must be imposed; the more severe will govern.

REFERENCES

1. T. R. Brussat, K. Kathiresan and T. M. Hsu, "Advanced Life Analysis Methods - Cracking Data Survey and NDI Assessment for Attachment Lugs," AFWAL-TR-84-3080, Vol. I, Air Force Wright Aero. Lab., September 1984.
2. K. Kathiresan, T. M. Hsu and T. R. Brussat, "Advanced Life Analysis Methods - Crack Growth Analysis Methods for Attachment Lugs," AFWAL-TR-84-3080, Vol. II, Air Force Wright Aero. Lab., September 1984.
3. K. Kathiresan and T. R. Brussat, "Advanced Life Analysis Methods - Experimental Evaluation of Crack Growth Analysis Methods for Attachment Lugs," AFWAL-TR-84-3080, Vol. III, Air Force Wright Aero. Lab., September 1984.
4. K. Kathiresan and T. R. Brussat, "Advanced Life Analysis Methods - Tabulated Test Data for Attachment Lugs," AFWAL-TR-84-3080, Vol. IV, Air Force Wright Aero. Lab., September 1984.
5. K. Kathiresan and T. R. Brussat, "User's Manual for "LUGRO" Computer Program to Predict Crack Growth in Attachment Lugs," AFWAL-TR-84-3080, Vol. VI, Air Force Wright Aero. Lab., September 1984.
6. Anon., "Damage Tolerance Design Requirements," Military Specification MIL-A-83444 (USAF), Air Force Aeronautical Systems Division, March 1973.
7. J. E. Collipriest, Jr. and R. M. Ehret, "Computer Modeling of Part-Through Crack Growth," SD 72-CE-00158, Space Division, Rockwell Int. Corp., October 1973.
8. T. McCann, Jr. and E. L. Caustin, "B-1 NDT Demonstration," presented at the Western Metal and Tool Exposition, Los Angeles, March 12, 1974.
9. R. J. H. Wanhill, A. A. Jongebreur, E. Morgan and E. J. Moolhuijsen, "Flight Simulation Fatigue Crack Propagation in Single and Double Element Lugs," NLR-MP-80023U, Nat. Aero. Lab., Amsterdam, The Netherlands, March 1981.
10. T. R. Brussat, S. T. Chiu and M. Creager, "Flaw Growth in Complex Structure," AFFDL-TR-77-79, Vol. I, Air Force Flight Dynamics Laboratory, December 1977.

11. J. L. Rudd, "Application of the Equivalent Initial Quality Method," AFFDL-TM-77-58-FBE, Air Force Flight Dynamics Laboratory, July 1977.
12. T. R. Brussat, "Estimating Initiation Times of Secondary Fatigue Cracks in Damage Tolerance Analysis," Fatigue of Engrg. Mat'ls. and Struct., Vol. 6, No. 3, 1983, pp. 281-292.